Volume 4 | Number 1 | January 2017

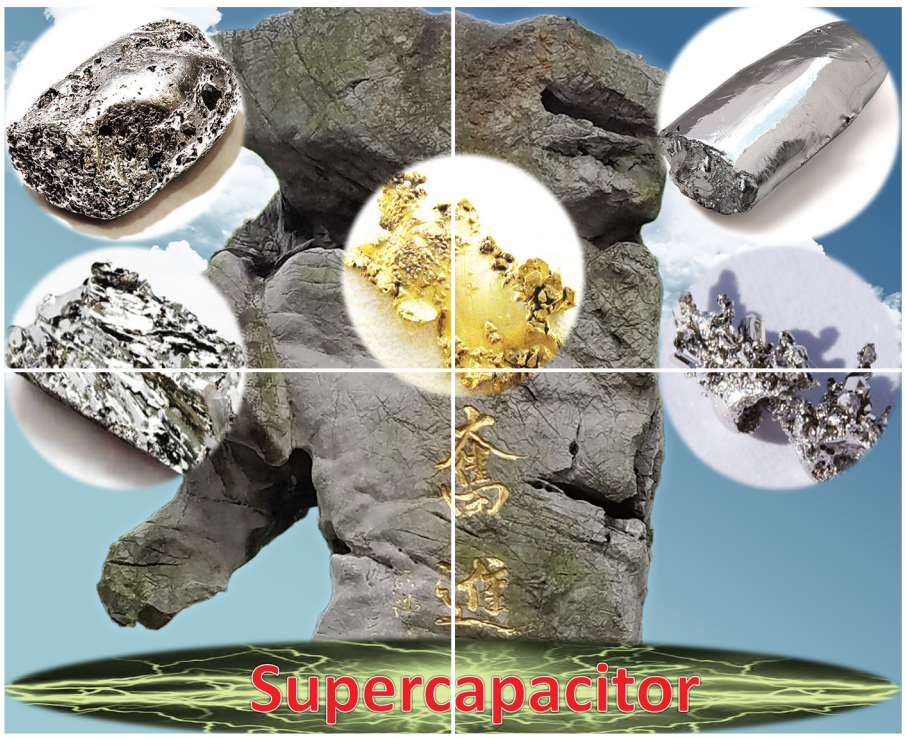

INORGANIC CHEMISTRY

FRONTIERS

Chinese Chemical Society
PEKING UNIVERSITY 1898
ROYAL SOCIETY OF CHEMISTRY

rsc.li/frontiers-inorganic

INORGANIC CHEMISTRY
FRONTIERS

REVIEW

View Article Online
View Journal | View Issue

Cite this: *Inorg. Chem. Front.*, 2017, **4**, 33

Noble metal-based materials in high-performance supercapacitors

Yan Yan,[a] Tianyi Wang,[a] Xinran Li,[a,b] Huan Pang*[a] and Huaiguo Xue*[a]

Received 23rd June 2016,
Accepted 1st October 2016

DOI: 10.1039/c6qi00199h

rsc.li/frontiers-inorganic

Noble metal-based materials have been intensively investigated as good additives of electrode materials for supercapacitors, since they can improve the specific capacitance, conductivity, and chemical and thermal stabilities of the electrode materials. This review carefully summarizes noble metal-based materials for high-performance supercapacitor electrodes. The advances of hybrid electrodes are then assessed to include hybrid systems of noble metal-based materials with compounds such as carbonaceous materials, metals and transition metal oxides or hydroxides. A variety of synthetic methods such as hydrothermal/solvothermal methods, polymerization, and electrodeposition methods are also discussed to prepare noble metal-based materials. This review comprehensively summarizes and evaluates the recent progress in the research on noble metal-based electrode materials for supercapacitors, including synthesis methods, electrochemical performances, and related devices.

1. Introduction

The world is facing an energy crisis that has arisen from people's significantly increased demand for energy, as traditional fossil fuels, including coal, oil and natural gas, have become rarer and more expensive to be viable candidates as energy sources.[1–3] It has been proven that the burning of fossil fuels has resulted in the increase of carbon dioxide, methane and other greenhouse gases, which poses a serious threat to the ecology of the earth.[4,5] With this background, it is high time that people develop renewable energy in place of traditional fossil fuels. The development of new energy is changing with each passing day, with a variety of energy storage devices such as solar cells, fuel cells, supercapacitors and rechargeable batteries.[6–9]

Among the various energy storage devices, supercapacitors are increasingly favored by researchers. Supercapacitors, also known as ultracapacitors or electrochemical capacitors, are energy storage devices that employ high surface area electrode materials and thin electrolytic dielectrics to achieve greater capacitances when compared to other energy storage devices such as batteries, fuel cells and conventional capacitors.[10–12]

[a]*College of Chemistry and Chemical Engineering, Yangzhou University, Yangzhou, 225002 Jiangsu, China. E-mail: panghuan@yzu.edu.cn, huanpangchem@hotmail.com, chhgxue@yzu.edu.cn*
[b]*College of Chemistry and Chemical Engineering, Anyang Normal University, Anyang, 455002, P. R. China*

Yan Yan

Yan Yan is now a Ph.D. candidate under Professor Huan Pang's and Huaiguo Xue's supervision, Yangzhou University of Chemistry and Chemical Engineering, China. His research mainly focuses on the field of electrochemistry, including inorganic semiconductor nanostructures, conducting polymers and their applications in energy devices.

Tianyi Wang

Tianyi Wang is currently a student under Professor Huan Pang's supervision in the Yangzhou University of Chemistry and Chemical Engineering, China. His research mainly focuses on the field of electrochemical energy storage materials and their applications.

The performance of supercapacitors mainly includes five aspects, including work voltage, specific capacitance, specific energy (energy density), specific power (power density) and cycle life.[13–18] The primary factor that affects the performance of supercapacitors is the electrode material. The preparation of electrode materials with stable performance and good electrical conductivity has been a hot research topic.[19–22]

The common electrode materials of supercapacitors include carbon based materials (activated carbon, carbon nanotubes, graphene, *etc.*), transition-metal oxides, conducting polymers and the composites formed from these materials.[23–25] Because of their good conductivity and electrochemical stability, noble metals have attracted extensive research in the field of electrode materials of supercapacitors.[26–29] Noble metals usually include the platinum group (ruthenium, rhodium, palladium, osmium, iridium, platinum), silver and gold.[30] Up to now, among the noble metals, only ruthenium, rhodium, palladium, platinum, silver and gold are involved in the research of electrode materials for supercapacitors. Due to their high conductivity, noble metals can facilitate effective transport of electrons that arise from the oxidation/reduction of pseudocapacitors to the current collectors.[31–33] However, due to the scarcity and high cost of noble metals, their integration with other sustainable and cheap materials is considered one of the most attractive ways to optimize their properties and minimize their consumption.

In this review, we carefully introduce different kinds of noble metal-based materials (silver, gold, platinum, and their related composites) in supercapacitors. Firstly, by comparing the electrode materials with and without a noble metal, we can find that the noble metal can significantly improve the performance of the supercapacitor, such as specific capacitance and cycling stability. What's more, there are also some reports on noble metals alone serving as the active materials for supercapacitor electrodes. Lastly, we provide some perspectives as to the future directions of this intriguing field and several possible research trends in noble metal-based materials for high performance supercapacitors.

2. Silver

Silver has the highest conductivity among the noble metals. Silver leads to nanoscale electrical contacts between the electrode and current collectors. Porous silver is one of the most important materials, especially for applications such as energy storage, surface-enhanced Raman scattering, and catalysis. Among the noble metal materials, Ag is very attractive due to its lower cost than other noble metals. Recently, Ag nanoparticles (AgNPs) have been used as conductive dopants in electrode materials for lithium-ion batteries and supercapacitors. Up to now, silver incorporated onto mesoporous carbon, carbon nanotubes, graphene, metal oxides, metal hydroxides, conducting polymers and their nanocomposites and other metallic silver based electrodes have been reported for supercapacitor applications.

2.1 Silver/metal oxide composites

A variety of methods can be used to prepare silver/metal oxide composites for supercapacitors such as cathodic electrolytic deposition, electrochemical dealloying, cathodic reduction methods, hydrothermal/solvothermal methods, and silver mirror reaction. Metal oxides, such as manganese oxides, nickel oxides, copper oxides, cobalt oxides and silver oxides, have been individually studied as electrode materials and yielded positive results. However, these metal oxides have poor electrical conductivity, which can have a detrimental influence on specific capacitance and cycling stability. Therefore, by combining these complementary metal oxides with silver, it was hoped to promote desirable synergistic properties and

Xinran Li

Xinran Li is now a student under Professor Huan Pang's supervision, Yangzhou University of Chemistry and Chemical Engineering, China. Her research mainly focuses on the field of micro/nanocoordination derived materials for electrochemical energy devices.

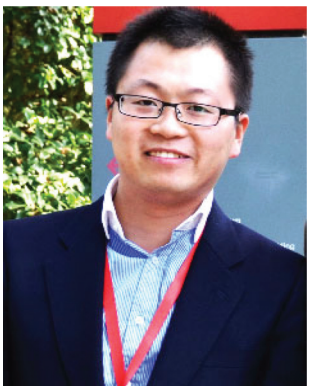

Huan Pang

Huan Pang received his Ph.D. degree from Nanjing University in 2011. He then founded his research group in Anyang Normal University where he was appointed as a distinguished professor in 2013. He has now joined Yangzhou University as a university distinguished professor. He has published more than 100 papers in peer-reviewed journals including Chem. Soc. Rev., Adv. Mater., *and* Energy Environ. Sci. *with 3600 citations (H-index = 32). His research interests include the development of inorganic nanostructures and their applications in flexible electronics with a focus on energy devices.*

Table 1 Comparison of the capacity and the corresponding test conditions of silver/manganese oxide composites in the literature

Material	Current collector	Electrolyte	Potential window (V)	Capacity (F g^{-1})	Capacity retention (%)
Ag-doped MnO_2 films[31]	Stainless steel foil	0.5 M Na_2SO_4	0–0.9 (SCE)	770 (2 mV s^{-1})	—
Nanoporous silver/MnO_2 [32]	Nanoporous silver	2 M Li_2SO_4	0–0.8 (Ag/AgCl)	1088 (1 A g^{-1})	—
Ag/MnO_2 nanowires[33]	Ti foil	1 M Na_2SO_4	0–1.0 (Ag/AgCl)	293 (10 mV s^{-1})	96.8% (5000 cycles, 50 mV s^{-1})
Tubular Ag/MnO_x [34]	Nickel foam	1 M Na_2SO_4	0–1.0 (SCE)	180 (0.1 A g^{-1})	80% (1000 cycles, 1 A g^{-1})
Ag-doped fibrous MnO_x [35]	Carbon fibers	0.5 M Na_2SO_4	0–0.8 (Ag/AgCl)	825 (5 mV s^{-1})	~100% (1000 cycles, 3 A g^{-1})

functionalities and yield composites with improved capacitive performance.

Manganese oxides such as MnO_2, Mn_3O_4 and MnO_x are often used as electrode materials for supercapacitors due to their high specific capacitance. MnO_2 has different crystal phases, such as α-, β-, δ-, γ- and λ-, all of which contain MnO_6 octahedra that are a veritable type of "toolbox" with the ability to accommodate foreign cations, water molecules, or structural vacancies. This structural feature makes it easy to dope MnO_2 nanomaterials with metal nanoparticles and then to improve the electrical conductivity of MnO_2 and boost its performance. A comparison with previously reported silver/manganese oxide composites is given in Table 1.

Electrodeposition methods can be employed in the presence of template structures to replicate a wide variety of structures. Wang *et al.* prepared Ag-doped MnO_2 films by cathodic electrolytic deposition from a $KMnO_4$ aqueous solution containing $AgNO_3$, obtaining the highest specific capacitance of 770 F g^{-1} at a scan rate of 2 mV s^{-1}.[31] Xia and co-workers successfully prepared a hierarchical heterostructure of silver nanoparticle (AgNP)-decorated MnO_2 nanowires (shown in Fig. 1a) by using a facile yet efficient chemical protocol, decorating conductive silver nanoparticles (10 nm) on MnO_2 nanowires (width of 10–20 nm).[32] Their strategy was a simple one-pot method to prepare one dimensional hierarchical Ag/MnO_2 nanowires by simply immersing a Ag foil into a mixed solution of $KMnO_4$ and H_2SO_4. The electrode delivered a large specific capacitance (293 F g^{-1} at a scan rate of 10 mV s^{-1}), a good cycling performance (96.8% capacitance retention after 5000 cycles) (shown in Fig. 1b), and a high rate capability (with a specific energy and power density of 17.8 Wh kg^{-1} and 5000 W kg^{-1} at 10 A g^{-1}, respectively).

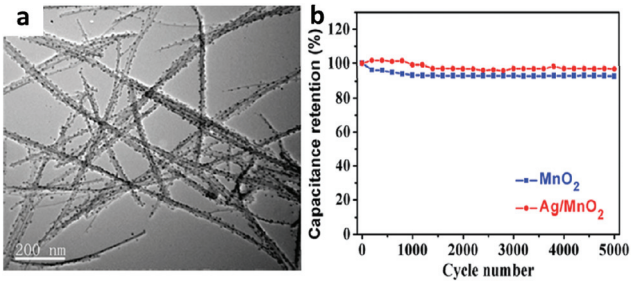

Fig. 1 (a) TEM image of silver nanoparticle (AgNP)-decorated MnO_2 nanowires; (b) cycling behavior of silver nanoparticle (AgNP)-decorated MnO_2 nanowires. Adapted with permission from ref. 32, © 2015 The Royal Society of Chemistry.

Li *et al.* successfully prepared 3D nanoporous silver (NPS)/MnO_2 composites *via* the electrochemical dealloying of $Ag_{45}Mg_{35}Ca_{20}$ metallic glass, followed by the electroless plating of nanocrystalline MnO_2.[33] The NPS/MnO_2 composite electrode provided fast ionic conduction and excellent electron–proton transport, resulting in an ultrahigh specific capacitance of the plated active MnO_2 (1088 F g^{-1} at 1 A g^{-1}).

The Kirkendall effect is an effective method for the fabrication of hollow nanostructures and nanocomposites. Li's group synthesized one-dimensional (1D) tubular Ag/MnO_x nanocomposites by the solvothermal method *via* the Kirkendall effect between potassium permanganate ($KMnO_4$) and Ag nanowire templates.[34] The hierarchical tubular Ag/MnO_x nanosheet composites exhibited an optimized electrochemical performance, with a specific capacitance of 180 F g^{-1} at a current density of 0.1 A g^{-1}, and still maintained 80% of the initial capacity after 1000 cycles at a current density of 1 A g^{-1}. Zeng *et al.* deposited Ag-doped manganese oxide on carbon fibers *via* a cathodic reduction method, then the deposits were dehydrogenized and oxidized by heat treatment at 350 °C for 4 h.[35] The doped Ag improved the electrochemical performance and the specific capacitance calculated is about 825 F g^{-1} at a scan rate of 5 mV s^{-1}.

NiO is an ideal pseudocapacitive material due to its high specific capacitance, good capability retention and especially environment-friendliness. Chemical bath deposition is a simple wet chemical technique to deposit wide varieties of thin films on various substrates. Wu *et al.* prepared highly porous NiO/Ag composite films (shown in Fig. 2a) by combining chemical bath deposition and silver mirror reaction.[36] The

Huaiguo Xue

Huaiguo Xue received his Ph.D. degree in polymer chemistry from Zhejiang University in 2002. He is currently a professor of physical chemistry and the dean of the College of Chemistry and Chemical Engineering at Yangzhou University. His research interests focus on electrochemistry, functional polymers and biosensors.

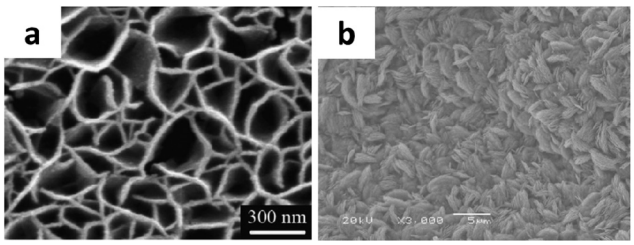

Fig. 2 (a) SEM image of a porous NiO/Ag composite film; (b) SEM image of a Ag-doped CuO nanosheet. (a) Adapted with permission from ref. 36, © 2011 Elsevier; (b) adapted with permission from ref. 37, © 2012 Elsevier.

specific capacitances of the NiO/Ag composite were 330 F g^{-1} at 2 A g^{-1} and 281 F g^{-1} at 40 A g^{-1}, which were much higher than the unmodified porous NiO film (261 F g^{-1} at 2 A g^{-1} and 191 F g^{-1} at 40 A g^{-1}). As another common pseudocapacitive material, CuO has many attractive features as NiO.

Huang *et al.* prepared Ag-doped CuO nanosheets (shown in Fig. 2b) *via* a template-free growth method and silver mirror reactions.[37] The Ag-doped CuO nanosheet electrode showed capacitances of 689 F g^{-1} at 1 A g^{-1} and 299 F g^{-1} at 10 A g^{-1}, respectively, compared to that of the unmodified CuO nanosheet arrays (418 F g^{-1} at 1 A g^{-1} and 127 F g^{-1} at 10 A g^{-1}). Co_3O_4 is widely used as an electrode material for supercapacitors. Wang *et al.* reported a novel method for the large-scale fabrication of porous bulk silver thin sheets (PSTS), which were used as highly conductive substrates for the growth of Co_3O_4 capacitive materials.[38] The synthesis started with synthesizing silver sponges *via* an *in situ* growth of NPs which assemble into networks. The sponges were pressed into thin sheets before etching in an acid. The resulting porosity was nearly homogeneous throughout the whole volume. The dependence on the acid concentration was investigated and the average pore diameter can be controlled in the range of 83–145 nm by the etching time. The PSTS/Co_3O_4 electrode with the optimized Co_3O_4 covering of the Ag network ligaments exhibited high specific capacitances of 1276 F g^{-1} at 1 A g^{-1} and still 986 F g^{-1} at 10 A g^{-1}.

Nanowires (NWs) are 1D nanostructures, which are perfect building blocks for functional nanodevices and represent the smallest dimension for efficient electron and exciton transport. Silver nanowires have potential applications as electrodes of electrochemical capacitors due to their excellent conductivity. Hu and co-workers synthesized silver nanowires on a large scale by using anodic aluminum oxide (AAO) films as templates with ethylene glycol as the reductant.[39] Ag_2O/Ag coaxial nanowires were formed by the incomplete electrochemical oxidation during the charge step. The maximum specific capacitance of 987 F g^{-1} was obtained at a charge–discharge current density of 5 mA cm^{-2}.

2.2 Silver/metal hydroxide composites

$Ni(OH)_2$ is an important member of the pseudocapacitor family due to its well defined redox activity and large specific surface area values. However, their low electrical conductivity limits further improvement of the electrochemical properties. Ag-Doped $Ni(OH)_2$ nanomaterials are expected to improve the conductivity of the electrode material and show a higher specific capacitance by forming electron transfer channels during the charge/discharge cycles. Ghosh *et al.* reported a Ag deposited $Ni(OH)_2$/graphene composite (shown in Fig. 3a) electrode for supercapacitor application.[40] It showed a maximum specific capacitance of 496 F g^{-1} at 1 A g^{-1} current density accompanying 93% specific capacitance retention at the end of 500 consecutive charge–discharge cycles. By the combination of chemical vapor deposition and a hydrothermal process, Lan *et al.* developed ultralight and flexible supercapacitor electrodes that were made of $Ni(OH)_2$ nanosheets doped with Ag nanoparticles/three-dimensional (3D) graphene (Ag/$Ni(OH)_2$/3DG) (shown in Fig. 3b).[41] The first step was to grow 3D graphene on nickel foam using a CVD technique, which was considered as the most effective way to fabricate graphene films with a large surface area and high quality. The second stage was the synthesis of the $Ni(OH)_2$ nanosheets doped with Ag on the as-prepared 3D graphene *via* a simple hydrothermal method. Electrochemical tests showed a high specific capacitance of 2167 F g^{-1} scaled to the total mass of the electrodes at 10 A g^{-1} current density, a good rate capability and an excellent cycling performance of 98% capacitance retention over 1000 cycles at 25 A g^{-1} current.

2.3 Silver/carbon material composites

Carbon materials have been widely used, because of the advantages of simple preparation, large specific surface area, good electrical conductivity and cycling stability. The composites based on carbon-based materials and noble metal nanoparticles do not show pseudocapacitive behavior but are expected to enhance the electrical double layer capacitance by providing larger electrochemically active materials.

Carbon nanotubes are the most representative nanostructured carbons with one dimensional tubular structures and exhibit outstanding physicochemical properties such as high electrical conductivity, high mechanical strength, high chemical stability, and high activated surface areas. Through dispersing multi-walled nanotubes (MWCNTs) and Ag nanoparticles in water with the assistance of sodium

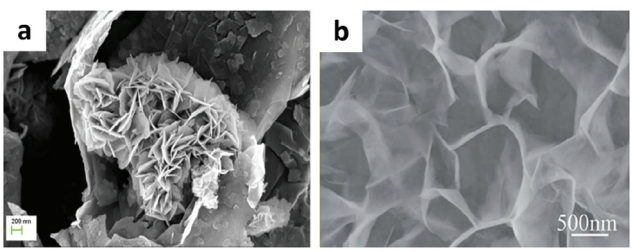

Fig. 3 (a) SEM image of a Ag@$Ni(OH)_2$/graphene composite; (b) SEM image of Ag/$Ni(OH)_2$/3DG. (a) Adapted with permission from ref. 40, © 2013 Elsevier; (c) adapted with permission from ref. 41, © 2015 The Royal Society of Chemistry.

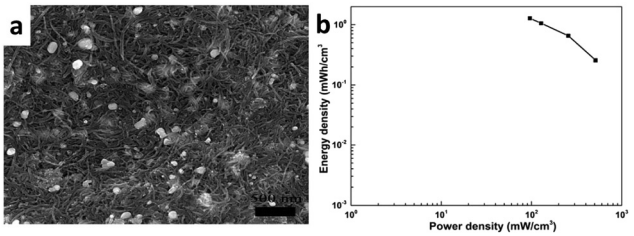

Fig. 4 (a) SEM image of a printed Ag-MWCNT conductive pattern; (b) Ragone plots of the asymmetric capacitor MnO_2-Ag-MWCNT/MWCNT. Adapted with permission from ref. 42, © 2015 The Royal Society of Chemistry.

dodecylbenzenesulfonate (SDBS), Wang *et al.* prepared a MWCNT and silver nanoparticle (shown in Fig. 4a) ink for inkjet printing.[42] Highly conductive patterns of Ag-MWCNTs were printed on paper using a HP Deskjet 1010 inkjet printer. The conductive patterns could act as a foldable electrical circuit. MnO_2–Ag-MWCNT anodes were also fabricated by inkjet printing. An asymmetric supercapacitor was fabricated by assembling an inkjet-printed MnO_2–Ag-MWCNT anode with a filtered MWCNT cathode. The supercapacitor had a wide operating potential window of 1.8 V and exhibited excellent electrochemical performance, a high density of 1.28 mWh cm^{-3} at a power density of 96 mW cm^{-3} (shown in Fig. 4b) and a high retention ratio of 96.9% of its initial capacitance after 3000 cycles.

As a new kind of carbon material, graphene has become an attractive low cost alternative for CNTs with the characteristics of high specific surface area, high electrical conductivity, and good mechanical properties. Using a simple vacuum filtration process, Shao *et al.* fabricated flexible, 3D, porous graphene/MnO_2 nanorods and graphene/Ag hybrid thin-film electrodes.[43] A novel asymmetric supercapacitor had been fabricated by using a graphene/MnO_2 nanorod thin film as the positive electrode and a graphene/Ag thin film as the negative electrode. The devices exhibited a maximum energy density of 50.8 Wh kg^{-1} and present a high power density of 90.3 kW kg^{-1}, even at an energy density of 7.53 Wh kg^{-1}.

Wee *et al.* designed a series of experiments to explore the particle size effect of silver nanoparticle decorated single walled carbon nanotube electrodes for supercapacitors.[44] The capacitance and energy density of the device can be doubled by decorating CNTs with AgNPs of 1 nm, which do not block the CNT network and complement the double layer capacitance by a faradaic reaction induced pseudocapacitance.

2.4 Silver/conducting polymer composites

As another important kind of pseudocapacitive material, recently, conducting polymer based composites and their application in the supercapacitors have been actively studied. Among these, polyanilines (PANI) have the advantages of a simple structure, small energy gap and high electrical conductivity, and have been widely used in energy storage materials. PANI/Ag composites used as electrode materials for supercapacitor applications are worthwhile to explore considering the highly electrically conductive Ag metal that may mediate the effective charge migration through the PANI. Patil *et al.* synthesized a Ag/PANI electrode by chemical polymerization *via* a simple and cost effective dip coating technique for supercapacitor application.[45] A specific capacitance of 512 F g^{-1} was observed at 5 mV s^{-1} and an energy density of 50.01 Wh kg^{-1} at 1 mA cm^{-2} was obtained for a PANI film having 0.9 weight percent Ag doping concentration.

Amarnath *et al.* synthesized water dispersible nanocomposite Ag@polyaniline-pectin (Ag@PANI-PEC), which exhibited electroactivity, specific capacitance (in physiological fluids) as well as reasonable biocompatibility and antibacterial properties.[46] The specific capacitances of Ag@PANI-PEC at a current density of 1.5 A g^{-1} were 140, 290, 144, and 121 F g^{-1} in phosphate buffer saline, blood, urine and serum, respectively. These results support that this nanocomposite may have commercial potential for environmentally friendly and inexpensive supercapacitor electrodes in biomedical applications. Zhang reported solid-state flexible aerogel supercapacitors that were fabricated from cellulose nanofibrils (CNFs), Ag and polyaniline nanoparticles.[47] The specific capacitance was calculated to be 176 mF cm^{-2} at 10 mV s^{-1}.

Polypyrrole (PPy) is an ideal electrode material for supercapacitors, which has high electrical conductivity, good environmental stability, reversible electrochemical redox properties and strong charge storage capacity. PPy–metal nanocomposites are widely investigated as electrode materials due to their excellent stability under environmental conditions, good conductivity, and biocompatibility. In recent years, a lot of methods have been employed for the preparation of PPY/silver composites either chemically or electrochemically for the study of their different properties and applications. Singh *et al.* report a facile route for the synthesis of free standing polypyrrole–silver (PPy–Ag) nanocomposite films by photopolymerization of pyrroles using $AgNO_3$ as a photosensitizer in aqueous medium.[48] The more conductive thin PPy–Ag films exhibited a low specific capacitance of 58 F g^{-1} compared to the specific capacitance of 282 F g^{-1} for the thicker PPy–Ag films at 1 mV s^{-1} scan rate. Wei *et al.* successfully demonstrated the one-step synthesis of PPy–Ag nanocomposites (shown in Fig. 5a) that were directly deposited on nickel foam by *in situ* polymerization.[49] The electrode showed outstanding pseudocapacitance behavior and good charge–discharge reversibility, and a specific capacitance of 493 F g^{-1} that was obtained at a current density of 1 A g^{-1} (shown in Fig. 5b).

Recently, Gan and co-workers demonstrated a facile strategy for the synthesis of hybrid Ag nanoparticle/nanocluster-decorated PPy nanocomposites, with an enhanced specific capacitance of 414 F g^{-1} and a remarkable cycling stability of 98.9% capacitance retention over 1000 charge–discharge cycles.[50] By chemical polymerization *via* a simple and cost effective dip coating technique, Patil *et al.* synthesized polypyrrole/polyacrylic acid (PAA)/silver composites (shown in Fig. 5c).[51] The highest specific capacitance of 226 F g^{-1} at 10 mV s^{-1} and an

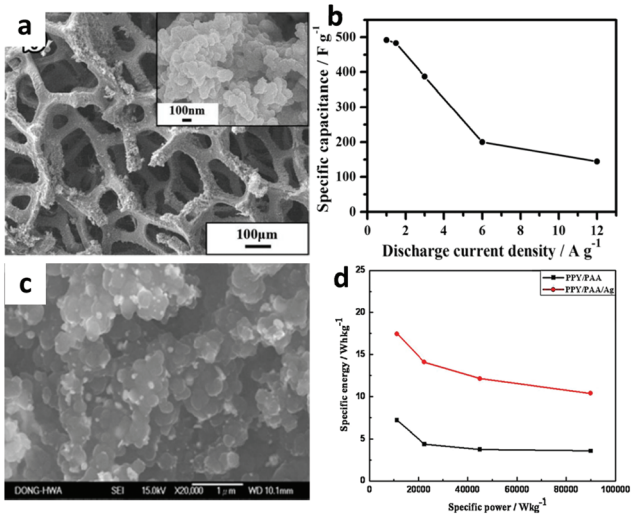

Fig. 5 (a) SEM image of PPy-Ag nanocomposite modified nickel foam; (b) specific capacitances at various discharge current densities of PPy–Ag nanocomposites; (c) SEM images of PPY/PAA/Ag composites; (d) Ragone plot of PPY/PAA and PPY/PAA/Ag at different current densities. (a, b) Adapted with permission from ref. 49, © 2013 The Royal Society of Chemistry; (c, d) adapted with permission from ref. 51, © 2013 Elsevier.

energy density of 17.45 Wh kg^{-1} at 0.5 mA cm^{-2} was obtained for the PPY/PAA/Ag composite electrodes (shown in Fig. 5d).

2.5 Silver containing ternary composites

Ternary composites have recently been employed as electrode materials to obtain better electrical performance. In these materials, each element contributes a much-needed function for energy based on carbonaceous materials. Ternary composites exhibit high specific capacitances, good rate capability, and good cycling stability. Thus, the combination of three elements can greatly improve the electrochemical performance of the composite electrode.

Reduced graphene oxide (RGO) has been incorporated with metal oxides to synthesize composite materials in order to improve the energy storage performance. Ma *et al.* demonstrated a two-step route to prepare ternary Ag/MnO_2/RGO nanocomposites with Ag and MnO_2 nanoparticles homogeneously deposited on the surface of RGO sheets.[52] The ternary nanocomposite of Ag/MnO_2/RGO, in which reduced graphene oxide sheets were decorated with Ag and MnO_2 nanoparticles, was synthesized by *in situ* growth of MnO_2 nanoparticles on graphene oxide sheets, followed by co-reduction of Ag^+ and GO. The Ag/MnO_2/RGO nanocomposites showed a specific capacitance as high as 467.5 F g^{-1} at a scan rate of 5 mV s^{-1}.

Ag/MnO_2 composites combined with conducting polymers have been proposed and investigated for use in supercapacitor electrodes. Using a pulsed potential electrodeposition technique, Kim synthesized ternary Ag/MnO_2/polyaniline (PANI) nanocomposite thin films without carbonaceous materials.[53] The specific capacitance of the ternary Ag/MnO_2/PANI nanocomposite is calculated to be 621 F g^{-1} and 800 F g^{-1} from CV and CD (charge–discharge) measurements, respectively. As a kind of aqueous polymer solution, poly(3,4-ethylenedioxythiophene):poly(styrenesulfonate):(PEDOT:PSS) has high conductivity. Using spin-coating, Yu and co-workers developed a sandwich-like Ag/PEDOT:PSS/MnO_2 layer by layer structure (shown in Fig. 6a) for high performance flexible supercapacitors.[54] This composite electrode provided an excellent specific capacitance of 862 F g^{-1} at a current density of 2.5 A g^{-1} and robust long-term cycling stability (shown in Fig. 6b).

As another kind of manganese oxide, Mn_3O_4 exhibits good electrochemical performance for supercapacitor applications. Through the starch assisted green chemistry method, Nagamuthu successfully synthesized silver incorporated Mn_3O_4/amorphous carbon (AC) nanocomposites.[55] The Ag–Mn_3O_4/AC electrode obtained a higher specific capacitance of 981 F g^{-1} at a specific current of 1 A g^{-1}.

CeO_2 can be selected as an electrode material for supercapacitors due to its low cost, good electrochemical characteristics, and surface dependent catalytic properties. Hydrothermal or solvothermal synthesis is a group of methods to crystallize inorganic substances from aqueous (thus named hydrothermal) or organic (thus named solvothermal) solutions at elevated vapour pressures and temperatures. Vanitha *et al.* synthesized a novel ternary Ag decorated CeO_2/RGO nanocomposite *via* a facile hydrothermal method with polyvinylpyrrolidone (PVP) as a surface directing agent.[56] The nanocomposite electrode materials possessed a high specific capacitance of 710.42 F g^{-1} at an applied current density of 0.2 A g^{-1}.

Zhi *et al.* developed highly conductive ordered mesoporous carbon based electrodes that were decorated with 3D graphene and 1D silver nanowires for flexible supercapacitors.[57] The flexible electrodes exhibited excellent long-term stability with >90% capacitance retention over 10 000 cycles, as well as a high energy and power density (4.5 Wh kg^{-1} and 5040 W kg^{-1}, respectively). Lee *et al.* developed carbon nanotube (CNT)/silver nanowire (AgNW) composite electrodes for flexible supercapacitors.[58] The supercapacitors which used CNT/AgNWs as electrodes demonstrated stable charging–discharging operation over 3000 cycles and low internal resistance.

Carbon material/conducting polymer composites have been widely used in the field of supercapacitors. It is viable to improve the performance of the supercapacitor by the combi-

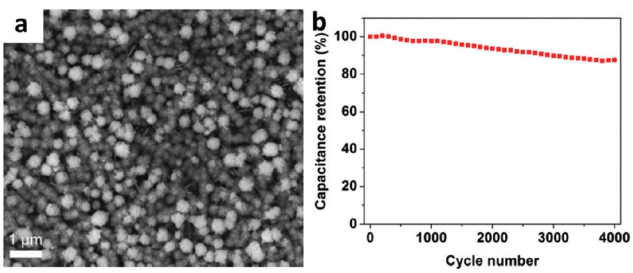

Fig. 6 (a) SEM images of sandwich-like Ag/PEDOT:PSS/MnO_2; (b) cycling behavior of sandwich-like Ag/PEDOT:PSS/MnO_2. Adapted with permission from ref. 54, © 2014 The Royal Society of Chemistry.

nation of silver, carbon materials and conducting polymers at the same time. Recently, carbon/PANI composites have attracted considerable attention as electrode materials due to the combination effect of both PANI and carbon. Patil's group demonstrated the electrochemical performance of a silver-activated carbon (AC)/polyaniline (shown in Fig. 7a) electrode prepared by deposition on stainless steel substrates by a facile dip coating technique.[59] The AC/PANI composite was prepared by *in situ* chemical oxidative polymerization of the corresponding aniline monomer and silver nanoparticles incorporated into the AC/PANI composite. The highest specific capacitance of 567 F g^{-1} at 5 mV s^{-1} and energy density of 86.30 Wh kg^{-1} at 1 mA cm^{-2} were observed for the Ag-AC/PANI indicating the positive synergistic effect of silver, activated carbon and PANI.

In recent times many efforts have been focused on the synthesis of Ag–PANI/CNT composites, using various synthetic procedures and being analyzed by different characterization techniques. By a simple and inexpensive *in situ* oxidative polymerization technique, Dhibar *et al.* successfully prepared a high-performance electrode material based on Ag nanoparticles decorated on PANI coated A-MWCNTs (shown in Fig. 7b).[60] The nanocomposites achieved the highest specific capacitance of 528 F g^{-1} at 5 mV s^{-1} scan rate. The nanocomposite also attained a better energy density of 187.73 Wh kg^{-1} and power density of 4185 W kg^{-1} at 5 mV s^{-1} and 200 mV s^{-1} scan rates, respectively. By *in situ* polymerization, Kim *et al.* prepared core/shell Ag–graphite nanofibers (GNFs)/PANI composites (shown in Fig. 7c) as electrode materials for supercapacitors.[61] The highest specific capacitance (212 F g^{-1}) of the Ag–GNFs/PANI was obtained at a scan rate of 0.1 A g^{-1}.

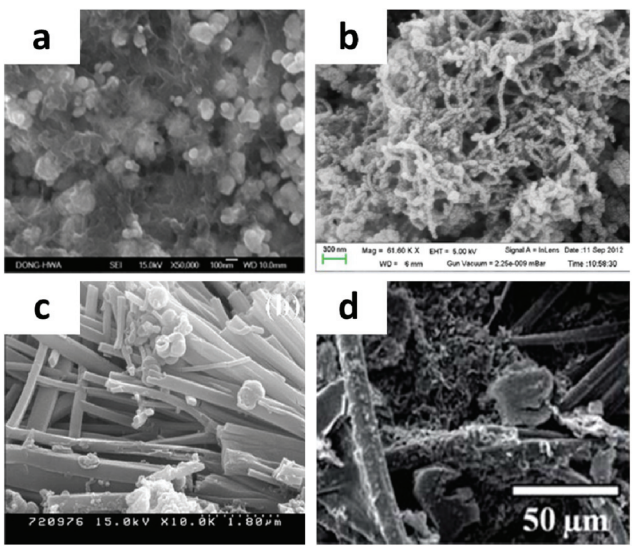

Fig. 7 SEM image of (a) silver-activated carbon/polyaniline; (b) silver-polyaniline/multiwalled carbon nanotubes; (c) polyaniline-coated Ag-GNFs; (d) AgNP–PANI–graphene nanocomposite. (a) Adapted with permission from ref. 59, © 2014 Elsevier; (b) ref. 60, © 2014 American Chemical Society; (c) ref. 61, © 2012 Elsevier; (d) ref. 62, © 2013 The Royal Society of Chemistry.

Recently, hybrid materials of PANI and graphene related materials have been recognized as potential ultrahigh capacitive electrode materials due to their incorporation of EDLC and pseudocapacitance effects. Sawangphruk *et al.* prepared a nanocomposite of AgNP–PANI–graphene (shown in Fig. 7d) *via in situ* polymerization.[62] The nanocomposite of AgNP–PANI–graphene in a weight ratio of 0.1 : 1 : 1, coated on flexible carbon fiber paper (CFP), exhibited high specific capacitance and capacity retention. At an applied current density of 1.5 A g^{-1}, the maximum specific capacitance of AgNP–PANI–graphene/CFP was 828 F g^{-1}. The capacity retention of AgNP–PANI–graphene/CFP after a charge–discharge test having 3000 cycles was 97.5% of the original specific capacitance.

Kalambate *et al.* synthesized graphene nanosheets (GNS)/AgNP/PPY nanocomposites using an *in situ* polymerization method.[63] GNS/AgNP/PPY exhibited a specific capacitance of 450 F g^{-1} at a current density of 0.9 mA g^{-1}. Furthermore, GNS/AgNP/PPY showed high charge–discharge reversibility retaining over 92.0% of its initial value after 1000 cycles.

2.6 Other silver containing materials

A conducting composite that consisted of polyacrylamide and Ag micro-powder (polyacrylamide/Ag composite) was prepared and its conductivity was determined. Through the free radical polymerization of an acrylamide monomer using *N*,*N*-methylene-bisacrylamide as the cross linker, and potassium persulfate as the initiator, Adelkhani *et al.* synthesized a polyacrylamide/Ag composite electrode, obtaining the highest specific capacitance of 950 F g^{-1}.[64] Naikoo *et al.* prepared porous silver (pAg) monoliths through a simple method for exploiting soft template Pluronic P123 (P123) and silica nanoparticles *via* a modified sol gel approach.[65] Electrochemical measurements showed that the maximum specific capacitance, power density and energy density obtained for pseudocapacitors using a pAg modified glassy carbon electrode (pAg/GCE) were 224.0 F g^{-1}, 17.6 kW kg^{-1} and 31.0 Wh kg^{-1}, respectively. Furthermore, pAg/GCE exhibited an excellent life cycle with 91.3% of its initial specific capacitance retained after 1000 cycles.

3. Gold

Like silver, gold is also widely used in supercapacitor electrode material systems. Incorporation of gold into electrodes can increase the specific capacity of metal-embedded electrodes, due to its high conductivity, stability and flexibility. The role of Au nanoparticles is not only to improve the electrical conductivity but also to enhance the structural stability. Au has been widely applied in many fields including fuel cells, electroanalysis and supercapacitors. Since Au is a precious and rare metal, there is an increasing demand for the preparation of highly active Au-based materials. Many reports have proved that the incorporation of Au with other materials, such as metal oxides, activated carbon and polymers, is one of the most attractive ways to achieve this goal.

Table 2 Comparison of the capacity and the corresponding test conditions of gold/manganese oxide composites in the literature

Material	Current collector	Electrolyte	Potential window (V)	Capacity (F g^{-1})	Capacity retention (%)
Au-doped MnO_2 films[66]	Nanoporous gold sheets	2 M Li_2SO_4	0–0.9 (Ag/AgCl)	626 (5 mV s^{-1})	93% (15 000 cycles, 50 mV s^{-1})
MnO_2-modified nanoporous gold wires[67]	Gold wires	1 M Na_2SO_4	0–0.8 (Ag/AgCl)	839.4 (0.5 mA cm^{-2})	90% (2000 cycles, 0.6 mA cm^{-2})
MnO_x/Au multilayers[68]	Au multilayers	1 M Li_2SO_4	0–0.8	—	74.1% (15 000 cycles, 1 V s^{-1})
MnO_2/Au/MnO_2 nanospike arrays[69]	Alumina NSPs	1 M Na_2SO_4	0–0.8 (Ag/AgCl)	—	88% (5000 cycles, 100 mV s^{-1})
Nanosized MnO_2 spines on Au[70]	Au nanowires	1 M Na_2SO_4	0–0.8 (Ag/AgCl)	1130 (2 mV s^{-1})	90% (5000 cycles, 10 A g^{-1})
MnO_2 nanorod Au nanoparticles[71]	Nickel foam	1 M Na_2SO_4	0–1.0 (Ag/AgCl)	406.8 (50 mV s^{-1})	91.3% (2000 cycles, 5 A g^{-1})
Nano-porous gold/manganese oxide nanowires[72]	Nano-porous gold	PVA/H_2SO_4 gel	0–0.8 (SCE)	—	81% (1000 cycles, 0.2 mA cm^{-2})
Manganese oxides/Au[73]	ITO glass	0.1 M KNO_3	0–1.0 (SCE)	1230 (20 mV s^{-1})	—

3.1 Gold/metal oxide composites

Coating the redox-active transition-metal oxides with a conductive metal layer is one efficient approach to improve the electrical conductivity of the oxide-based electrodes, which could largely boost the energy density and power density of supercapacitors.

A comparison with previously reported gold/manganese oxide composites is given in Table 2. Chen *et al.* developed novel Au-doped MnO_2 films that can be achieved by doping Au atoms into nanocrystalline λ-MnO_2 through sputter coating.[66] The resultant thick Au-doped MnO_2 films possessed an ultrahigh specific capacitance (626 F g^{-1} at a scan rate of 5 mV s^{-1}) and excellent cycling stability (7% increment after 15 000 cycles).

The nanoporous hybrid architecture, excellent conductivity and high flexibility of nanoporous gold (NPG) can provide superior electronic/ionic conductivity and mass transport giving enhanced performance. Xu *et al.* successfully designed and fabricated an all-solid-state, highly flexible, coaxial fiber asymmetric supercapacitor operated at 1.8 V by using an as-formed flexible NPG@MnO_2 hybrid as the core electrode and CNTs on carbon paper as the sheath electrode.[67] It showed excellent flexibility and performance including high capacitance and energy density (12 mF cm^{-2} and 5.4 μWh cm^{-2}) and excellent cycling stability (90% capacitance retention after 2000 cycles).

Yan's group introduced a new concept to fabricate on chip, all solid-state and flexible micro-supercapacitors based on MnO_x/Au multilayer electrodes.[68] The micro-supercapacitor exhibited a maximum energy density of 1.75 mWh cm^{-3} and a maximum power density of 3.44 W cm^{-3} and obtained a volumetric capacitance of 32.8 F cm^{-3} at a scan rate of 1 V s^{-1}. Through a low voltage anodization process, Gao *et al.* reported a unique supercapacitor structure based on ultra-thin, free-standing 3-D gold nanospike (NSP) films.[69] They fabricated the all solid-state symmetric supercapacitors based on MnO_2/Au/MnO_2 NSP (MAMNSP) (shown in Fig. 8a) electrodes. The systematic performance characterization showed that the devices have a high volumetric capacitance of 20.35 F cm^{-3} and a specific energy of 1.75×10^{-3} Wh cm^{-3}.

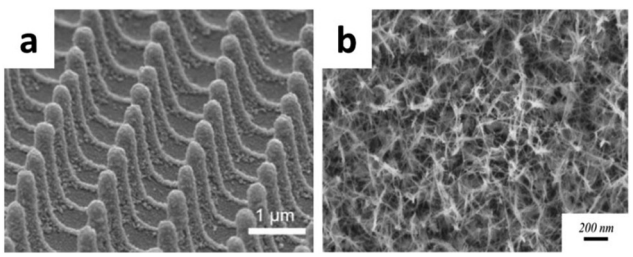

Fig. 8 SEM image of (a) MnO_2/Au/MnO_2 NSP; (b) manganese oxide nanowires on nano-porous gold; (c) Au–MnO_2–graphene composite; (d) Au–MnO_2/CNT hybrid coaxial nanotubes. (a) Adapted with permission from ref. 69, © 2015 The Royal Society of Chemistry; (b) ref. 72, © 2015 Elsevier.

Through simple electrochemical depositions, Chen *et al.* demonstrated a facile process to fabricate nanosized MnO_2 spines on Au stems (NMSAS) on flexible PET substrates for supercapacitor electrodes.[70] The maximum specific capacitance was determined to be 1130 F g^{-1} by cyclic voltammetry (CV, scan rate 2 mV s^{-1}) using a three-electrode system. The flexible electrodes also exhibited a maximum specific energy of 15 Wh kg^{-1} and a specific power of 20 kW kg^{-1} at 50 A g^{-1}. After five thousand cycles at 10 A g^{-1}, 90% of the original capacitance was retained.

Using a two-step procedure, Dai *et al.* fabricated MnO_2 nanorod Au nanoparticle composites that exhibited superior supercapacitance and long-term durability.[71] The composites have a specific capacitance of 406.8 F g^{-1} at a scan rate of 50 mV s^{-1}. The composites have 91.3% capacitance retention over 2000 charge–discharge cycles at 5 A g^{-1}. Zeng *et al.* prepared an all-solid-state nano-porous gold (NPG)/manganese oxide nanowire (shown in Fig. 8b) based interdigitated type micro-supercapacitor in a way that combined the micro fabrication and anodic electrodeposition processes.[72] It exhibited good electrochemical performance with a power density of 3.4 W cm^{-3} and an energy density of 50 mWh cm^{-3}.

By electrodeposition on an ITO glass substrate using a potentiostatic method in $KMnO_4/AuCl_3$ aqueous solution, Hu's group developed manganese oxide/Au nanocomposite thin films for supercapacitors.[73] The electrodes with 0.8% Au showed excellent capacitive behavior in the 0.1 M KNO_3 electrolyte, with the highest specific capacitance of 1230 F cm^{-3} at a scan rate of 20 mV s^{-1}. Qiu and co-workers developed a novel Au@MnO_2 core–shell nanomesh structure on a flexible polymeric substrate through nanosphere lithography combined with electrodeposition processing.[74] A high areal capacitance of 4.72 mF cm^{-2} and an ultrahigh rate capability up to 50 V s^{-1} had been achieved on Au@MnO_2 hybrid films.

Qu *et al.* presented a simple solution method to synthesize Au-decorated hierarchical NiO nanostructures (Au–NiO) (shown in Fig. 9a).[75] As a pseudocapacitor electrode, Au–NiO exhibited not only a remarkable cycling stability of 690 F g^{-1} at 4 A g^{-1} after 2000 cycles, but also an excellent rate capability of 619 F g^{-1} at 20 A g^{-1} (shown in Fig. 9b). Liu *et al.* synthesized monodispersed dumbbell-like Au–Fe_3O_4 nanoparticles for supercapacitors.[76] The dumbbell NPs show Au/Fe_3O_4-size dependent capacitive behaviors and the 7–14 nm Au–Fe_3O_4 NPs have the best specific capacitance of 464 F g^{-1} at 1 A g^{-1} and capacity retention of 86.4% after 1000 cycles.

Using a newly developed electrochemical partial dealloying–stripping method, Xu *et al.* successfully fabricated a novel nanoporous Au/AgO composite (NPAAC) with ligament-channel sizes of 10 nm.[77] The NPAAC revealed a superior cycling performance compared to metal-based pseudocapacitors, with stable charge–discharge cycling at 77 F g^{-1} for more than ten thousand times with no detectable degradation. By the electrospinning method followed by calcination in air, Zhu *et al.* synthesized novel $NiCo_2O_4$@Au nanotubes (NTs) with a mesoporous structure and hollow interiors.[78] The specific capacitance of $NiCo_2O_4$@Au NTs reached 1013.5 F g^{-1} and can be maintained at 85.13% after 10 000 cycles.

3.2 Gold/metal hydroxide composites

$Ni(OH)_2$ is a promising alternative electrode material not only because it is inexpensive and environmentally friendly but also because it presents very high theoretical specific capacitance. However, it suffers from poor conductivity, which makes it difficult to reach the theoretical capacitance of $Ni(OH)_2$, from poor rate capability, and from poor cycle stability. A possible way to improve the conductivity of poorly conducting $Ni(OH)_2$ is to incorporate a highly conductive metal such as Au into pseudocapacitor materials.

By a simple deposition of gold nanoparticles, Kim *et al.* reported a straightforward method to improve the performance of $Ni(OH)_2$ nanostructures (shown in Fig. 10a and b).[79] Compared with pristine $Ni(OH)_2$, Au/$Ni(OH)_2$ showed a 41% enhanced capacitance value, excellent rate capacitance

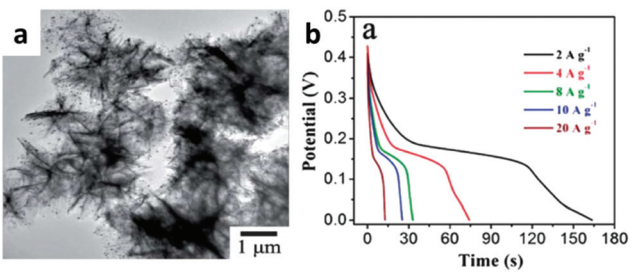

Fig. 9 (a) TEM image of Au–NiO hierarchical structures; (b) discharge voltage profiles of Au–NiO at different current densities; (c) SEM images of ZnO–Au–NiO hybrid composites; (d) galvanostatic discharge curves for ZnO–NiO and ZnO–Au–NiO electrodes at various current densities of 2, 5, 10, and 20 mA cm^{-2}. Adapted with permission from ref. 75, © 2013 The Royal Society of Chemistry.

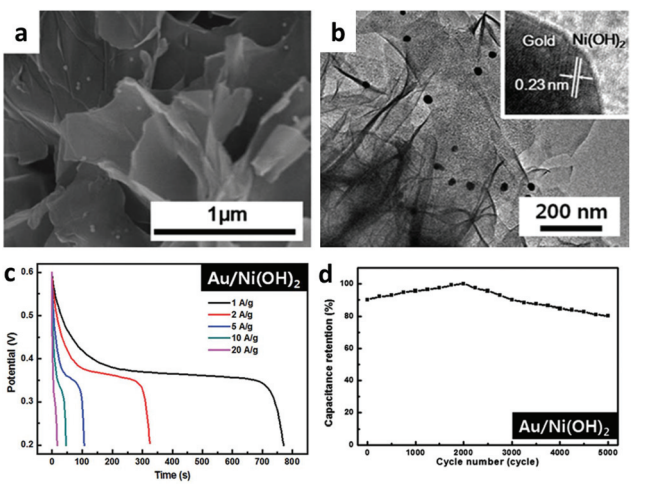

Fig. 10 (a) SEM image of Au/$Ni(OH)_2$ nanostructures; (b) TEM image of Au/$Ni(OH)_2$ nanostructures; (c) discharge voltage profiles of Au/$Ni(OH)_2$ at different current densities; (d) cycling behavior of Au/$Ni(OH)_2$ measured at 20 A g^{-1}. Adapted with permission from ref. 79, © 2014 The Royal Society of Chemistry.

behavior under high current density conditions, and greatly improved cycling stability for supercapacitor applications. The specific capacitance of Au/$Ni(OH)_2$ reached 1927 F g^{-1} at 1 A g^{-1} (shown in Fig. 10c), which was close to the theoretical capacitance and retained 66% and 80% (shown in Fig. 10d) of the maximum value at a high current density of 20 A g^{-1} and 5000 cycles while that of pristine $Ni(OH)_2$ was 1363 F g^{-1} and significantly decreased to 48% and 30%, respectively. The poor conductivity and stability of $Ni(OH)_2$ were addressed by introducing an appropriate metal/semiconductor contact, leading to improved rate capability and cycling stability capacitance as well as enhanced capacitance. The excellent performance of Au NP/$Ni(OH)_2$ is attributed to the creation of a unique 3D conductive nanoarchitecture due to the presence of Au metal NPs on the surface of the $Ni(OH)_2$ semiconductor, facilitating the transport of electrons or charge and ensuring enhanced catalytic activities.

Kim *et al.* developed an outstanding supercapacitor with a high capacitance, high energy density, and semipermanent lifetime using the $Ni(OH)_2$/NPG electrode.[80] The $Ni(OH)_2$/NPG electrode was optimized by finely adjusting the portion of two different parts of the deposited $Ni(OH)_2$, one part in direct contact with the NPG and the other part on top of the NPG. The optimized $Ni(OH)_2$/NPG electrode exhibited 2223 F cm^{-3} of volumetric capacitance (considering both the active material and the current collector) at a current density of 5 A g^{-1} and the device retained 90% capacitance of the initial value at 500 A g^{-1} and after 30 000 cycles, respectively.

3.3 Gold/carbon material composites

CNTs are the most representative nanostructured carbons with one dimensional tubular structures and exhibit outstanding physicochemical properties such as high electrical conductivity, high mechanical strength, high chemical stability, and high activated surface areas. Chaudhari *et al.* prepared Au-multiwall carbon nanotube (Au-MWCNT) composites with well-dispersed Au-nanoparticles using a simple and efficient solution method which were applied as electrode materials for electrochemical capacitors.[81] Au NP decoration boosts the supercapacitor performance of the Au-MWCNT composite compared with bare MWCNTs. The composite with a lower loading of 10 wt% Au displayed a higher specific capacitance (105 F g^{-1}) compared with bare MWCNTs (48 F g^{-1}) at a current density of 0.8 A g^{-1}.

Graphene is considered to be an excellent electrode material for supercapacitors due to its high electrical conductivity, high surface area, great flexibility, excellent mechanical properties, and rich chemistry. Ankamwar *et al.* prepared graphene-gold nanocomposites chemically from graphene oxide obtained from graphite oxide.[82] The nanocomposites were used as the electrode material in a low cost and environmentally-friendly supercapacitor device. It exhibited stable specific capacitance values of 100 and 500 F g^{-1} for the nanocomposite electrodes synthesized chemically and using gamma radiation, respectively, which remained constant over a potential scan rate of 5–500 mV s^{-1}. The fabricated electrode in the supercapacitor device exhibited excellent long cycle life along with the retention of 90% specific capacitance value after 600 cycle tests.

By the electrochemical reduction of GO at an indium tin oxide (ITO) electrode followed by an electrodeposition process of loading AuNPs on its surface, Yu synthesized a reduced graphene oxide–gold nanoparticle nanocomposite (RGO–AuNPs).[83] The performance of RGO–AuNPs showed a reversible electrochemical property and could be successfully applied as pseudocapacitor electrodes with an outstanding stability. A high specific capacity of 288 F g^{-1} at a high current density of 28 A g^{-1} was obtained in the electrochemical investigation.

Mandal *et al.* demonstrated the fabrication of a flexible supercapacitor using gold nanoparticles embedded in a paper with controlled mechanically exfoliated graphite electrodes.[84] A very high specific capacitance of 790 mF cm^{-2} at a scan rate of 5 mV s^{-1} was found for these simple paper–pencil based devices. The device was tested for reliability up to 5000 cycles. The maximum volumetric energy and power density are 3.617 mWh cm^{-3} and 68.514 mW cm^{-3}, respectively.

3.4 Gold/conducting polymer composites

PANI is one of the most promising electronically conducting polymers with potential applications as ECs because of its easy synthesis, high stability, and good conductivity. The addition of PANI can be either chemical or electrochemical. Lang *et al.* developed three-dimensional bicontinuous nanoporous Au/PANI composite films by one-step electrochemical polymerization of PANI shells onto dealloyed nanoporous gold (NPG) skeletons for applications in supercapacitors.[85] The NPG/PANI based supercapacitors exhibited an ultrahigh volumetric capacitance (1500 F cm^{-3}) and energy density (0.078 Wh cm^{-3}).

Ye's group introduced a simple and rapid fabrication method involving laser printing technology and *in situ* anodic electropolymerization to fabricate interdigital Au/polyaniline network hybrid electrodes on polyethylene terephthalate films for flexible, in-plane, and all-solid-state micro-supercapacitors.[86,87]

Reddy *et al.* developed an assembly of poly(*N*-methyl pyrrole) (PMP) doped with poly(3-styrene sulfonate) with embedded Au nanoparticles (PMP/Au) that was grown by electropolymerization of the monomer (MP) followed by adsorption of a Au colloid.[88] The supercapacitor with a novel asymmetric architecture comprising a pseudocapacitive poly (*N*-methyl pyrrole)/Au electrode and an electrical double-layer capacitive poly(*m*-aminobenzenesulfonic acid)-functionalized MWCNT electrode showed a specific capacitance of 967 F g^{-1}.

3.5 Gold containing ternary composites

Recently, ternary composites have attracted extensive attention of researchers due to their respective advantages to improve the comprehensive performance of materials. Ternary composites of carbon materials, conducting polymers, transition

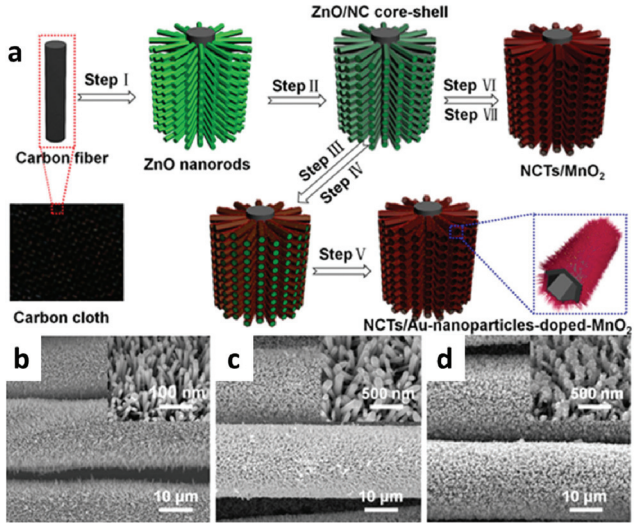

Fig. 11 (a) Schematic illustration of the fabrication of NCT/ANPDM nanocomposite on the carbon fabric substrate; (b–d) SEM images of ZnO nanorod arrays, ZnO/NC core–shell nanorod arrays, and NCT/ANPDM nanocomposite arrays grown on the carbon fabric. Adapted with permission from ref. 89, © 2016 American Chemical Society.

metal oxides and noble metals can combine their advantages and thus obtain improved electrochemical properties.

Using electrodeposition to grow an N-doped carbon-tube/Au-nanoparticle-doped-MnO_2 (NCT/ANPDM) nanocomposite on carbon fabric (shown in Fig. 11), Wang's group developed an advanced integrated electrode for high-performance pseudocapacitors.[89] A prototype solid-state thin-film symmetric supercapacitor (SSC) device based on NCT/ANPDM exhibited a large energy density (51 Wh kg^{-1}) and superior cycling performance (93% after 5000 cycles).

Wang and co-workers designed and fabricated a ternary graphene/Au/PANI nanocomposite (GAP) through a facile two-step approach: Au nanoparticles dispersed on graphene sheets are achieved by a hydrothermal method, followed by coating with PANI through an *in situ* polymerization process.[90] Electrochemical measurements demonstrated that the specific capacitance of the resulting ternary composite was 572 F g^{-1} at a current density of 0.1 A g^{-1} using a three-electrode system. In addition, over 88.54% of the initial capacitance can be retained after repeating tests for 10 000 cycles.

Veeramani *et al.* synthesized novel nanocomposite film Au–MnO_2–graphene (shown in Fig. 12a) *via* a two-step procedure involving electrophoretic and electrochemical deposition methods.[91] The supercapacitor provided a maximum capacitance of up to 575 F g^{-1} at a discharge current density value of 2.5 A g^{-1}. Reddy *et al.* synthesized Au–MnO_2/CNT hybrid coaxial nanotube arrays (shown in Fig. 12b) by the combination of electrodeposition, vacuum infiltration, and CVD techniques using porous alumina templates.[92] The Au–MnO_2/CNT hybrid coaxial nanotube electrodes showed excellent electrochemical performance with a maximum specific capacitance of 68 F g^{-1}, a power density of 33 kW kg^{-1}, and an energy density of 4.5 Wh kg^{-1}.

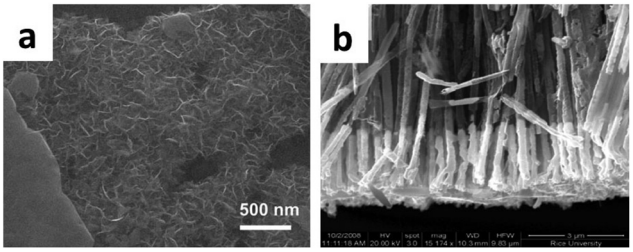

Fig. 12 (a) Au–MnO_2–graphene composite; (b) Au–MnO_2/CNT hybrid coaxial nanotubes. (a) Adapted with permission from ref. 91, © 2016 The Royal Society of Chemistry; (b) ref. 92, © 2010 American Chemical Society.

Han and co-workers synthesized conductive composite poly(*p*-phenylenediamine)/graphene oxide/Au (PPD/GO/Au) (shown in Fig. 13a) *via in situ* polymerization with *p*-phenylenediamine (PDA) used as a monomer and $HAuCl_4$ as an oxidant and Au source in the presence of graphene oxide (GO).[93] The maximum capacitance (238 F g^{-1}) of the composite which is obviously higher than 11 F g^{-1} of individual PPD and 176 F g^{-1} of PPD/GO can be obtained.

Shayeh developed polyaniline/reduced graphene oxide/Au nanoparticle (PANI/rGO/AuNP) composite (shown in Fig. 13b) electrodes that were deposited on a glassy carbon electrode (GCE) by the cyclic voltammetry (CV) method.[94] The specific capacitance of PANI/rGO/AuNP electrodes calculated using the CV method was 303 F g^{-1}.

Zhang *et al.* prepared a hierarchical MoO_2/Au/MnO_2 heterostructure *via* a two-step electrodeposition method.[95] The ion-diffusion and charge collection capacity improved after spraying an Au layer. Electrochemical tests show that the areal specific capacitance of MoO_2/Au/MnO_2 is up to 112 mF cm^{-2} at a scan rate of 5 mV s^{-1}. Zheng *et al.* designed a nanostructure by embedding Au nanoparticles into ZnO/NiO core–shell composites (shown in Fig. 14a) as supercapacitor electrode materials.[96] The ZnO–Au–NiO composites exhibited a maximum specific capacitance of 4.1 F cm^{-2} at a current

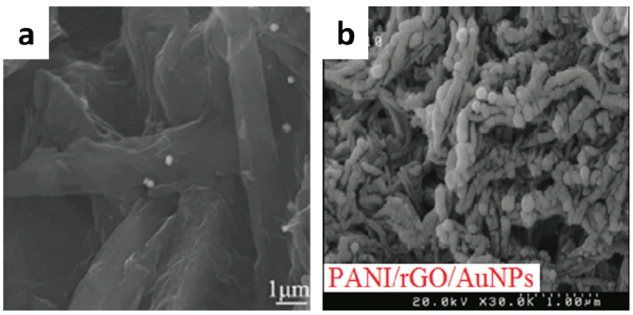

Fig. 13 SEM image of (a) PPD/GO/Au; (b) PANI/rGO/AuNPs. (a) Adapted with permission from ref. 93, © 2012 Elsevier; (b) adapted with permission from ref. 94, © 2015 Elsevier.

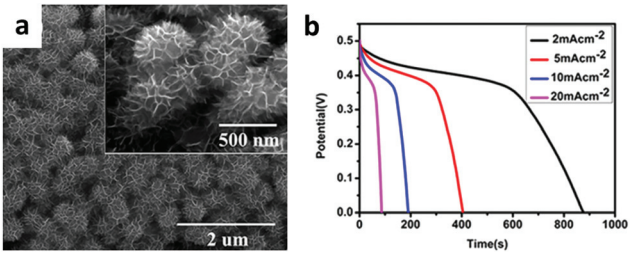

Fig. 14 (a) SEM images of ZnO–Au–NiO hybrid composites; (b) galvanostatic discharge curves for ZnO–NiO and ZnO–Au–NiO electrodes at various current densities of 2, 5, 10, and 20 mA cm^{-2}. Adapted with permission from ref. 96, © 2015 American Chemical Society.

density of 5 mA cm^{-2} (shown in Fig. 14b) and excellent stability (about 19.7% loss after 4000 cycles).

Wang's group developed hybrid WO_{3-x}@Au@MnO_2 core–shell nanowires on flexible carbon fabric (shown in Fig. 15).[97] Electrochemical measurements showed that the specific capacitance of these WO_{3-x}@Au@MnO_2 core–shell NWs reaches 588 F g^{-1} at a scan rate of 10 mV s^{-1} and 1195 F g^{-1} at a current density of 0.75 A g^{-1}. The WO_{3-x}@Au@MnO_2 core–shell NWs also exhibit excellent long-term cycling stability, a high power density of 30.6 kW kg^{-1} at an energy density of 78.1 Wh kg^{-1}, and an energy density of 106.4 Wh kg^{-1} at a power density of 23.6 kW kg^{-1}.

Wang *et al.* reported a solvothermal strategy and a mutual oxidation–reduction approach for the fabrication of RuO_2-based nanocomposites, including RuO_2/C and RuO_2–Au/C.[98] In particular, the as-prepared RuO_2/C and RuO_2–Au/C nanocomposites for supercapacitors adopting the H_2SO_4 electrolyte exhibited high specific capacitances of 537.7 F g^{-1} and 558.2 F g^{-1}, respectively, at a current density of 50 mA g^{-1}. The specific capacitance reaches 350.1 F g^{-1} for the RuO_2/C nanocomposites and 478.5 F g^{-1} for the RuO_2–Au/C nanocomposites at a current density of 200 mA g^{-1} with good cycling stability.

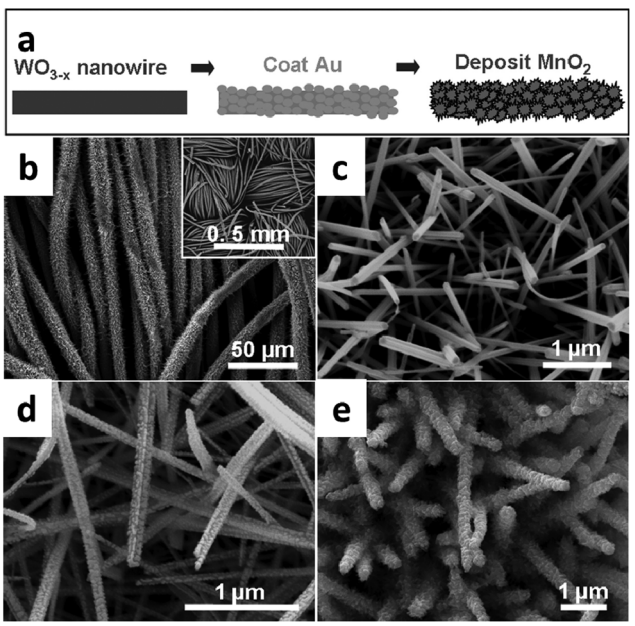

Fig. 15 (a) Schematic of the fabrication process for WO_{3-x}@Au@MnO_2 NWs; SEM images of the as-prepared (b, c) WO_{3-x} NWs on carbon fabric; (d) WO_{3-x}@Au NWs; (e) WO_{3-x}@Au@MnO_2 NWs on carbon fabric. Adapted with permission from ref. 97, © 2012 Wiley.

Very recently, Wang's group demonstrated a prototype ultrahigh performance Au-doped-α-MnO_2-ZnO-based electrode material based on low-cost and non-toxic metal nanocomposition according to first-principles calculations.[99] The doped Au atoms in the α-MnO_2 lattice and distributed Au nanoparticles in the α-MnO_2 nanothin layers can greatly enhance the conductivity and electrochemical performance of MnO_2. The designed carbon cloth electrodes modified with ZnO-nanorod/Au-doped-α-MnO_2 (ZN/ADM) nanocomposites exhibited excellent electrochemical performances. Moreover, an asymmetric supercapacitor based on ZN/ADM (positive) and reduced-graphene-oxide–CNTs (negative) hybrid materials demonstrated cycle reversibility in a wide potential window and exhibited high energy density (101 Wh kg^{-1}), power density (33.6 kW kg^{-1}), and reasonable cycling performance.

3.6 Other gold containing materials

Among metal phosphides, nickel phosphides have attracted much attention because they contain a number of phases, remarkable properties and potential applications. By a simple phosphorization process from the corresponding bimetallic heterostructures, Duan *et al.* synthesized Au/$Ni_{12}P_5$ core/shell nanoparticles and core/shell heterostructures.[100] The triphenylphosphine is designed to serve as both a capping agent and a phosphorus source during the formation of Au/$Ni_{12}P_5$ core/shell nanoparticles (NPs) from Au–Ni bimetallic heterodimers. The semiconductor shells of the obtained Au/$Ni_{12}P_5$ nanostructures are controlled to form single crystals with a thickness of 5 nm. The specific capacitance of the electrode fabricated from core/shell NPs was 806.1 F g^{-1} with a retention of 91.1% after 500 charge–discharge cycles.

The capacitive performance of the double-layer capacitors depends on the effective surface area and conductivity of electrode materials, conductive and porous inorganic materials, such as activated charcoal and other carbon nanomaterials. Nanoporous metals also have a large internal surface for charge storage and excellent conductivity required for high cycle efficiency and extremely low heat levels, which can offer better double-layer capacitive performance. Lang *et al.* reported the capacitive performances of a supercapacitor with three-dimensional nanoporous gold as electrodes.[101] The bicontinuous NPG with a large internal surface and high conductivity showed promising capacitive properties in both a conventional aqueous electrolyte and a green ionic liquid electrolyte. In comparison with the performance in the aqueous electrolyte, the NPG-based supercapacitor in the ionic liquid electrolyte showed higher energy density because of the high operation voltage arising from the low ionic mobility of the room-temperature ionic liquid.

Table 3 Comparison of the capacity and the corresponding test conditions of platinum-based materials in the literature

Material	Current collector	Electrolyte	Potential window (V)	Capacity (F g^{-1})	Capacity retention (%)
PtNP decorated graphene	Ni foam	6 M KOH	−1.0–0 (Hg/HgO)	154 (0.1 A g^{-1})	—
Graphene/Pt films	Pt	1 M H_2SO_4	0–1.0 (SCE)	120 (0.1 A g^{-1})	~100% (10 000 cycles, 50 mV s^{-1})
Multi-layer MnO_2/Pt nanophases,	Glassy carbon	0.5 M H_2SO_4	0–1.0 (Ag/AgCl)	252.3 (10 mV s^{-1})	93.5% (300 cycles, 10 mV s^{-1})
Pt-CNOs	Copper plate	0.1 M Na_2SO_4	−0.3–0.5 (Ag/AgCl)	837.4 (10 mV s^{-1})	~100% (2000 cycles, 20 A g^{-1})
Core/shell Pt/MnO_2 nanotubes.	Aluminium foil	1 M Na_2SO_4	0–0.9 (Ag/AgCl)	810 (5 mV s^{-1})	~100% (8000 cycles, 2 to 100 A g^{-1})
Co_3O_4/Pt	Pt	0.5 M H_2SO_4	0–1.0 (Ag/AgCl)	391.6 (100 mV s^{-1})	—
Co_3O_4@Pt@MnO_2 nanowire arrays	Ti foil	1 M Na_2SO_4	0–1.0 (Ag/AgCl)	539 (1 A g^{-1})	~100% (5000 cycles, 5 A g^{-1})
RuO_2-coated Pt fiber mats	Ti foil	1 M H_2SO_4	0–1.0	409.4 (10 mV s^{-1})	—
Pt/CNT@PANI nanowires	Pt filament	PVA/H_3PO_4 gel	0–1.0	—	80% (5000 cycles, 4 mA cm^{-2})
TiO_2–Pt@graphenes	—	1 M KOH	−0.5–0.5 (Ag/AgCl)	160 (5 mV s^{-1})	—

Gong *et al.* reported a simple yet efficient method to fabricate a self-assembled monolayer gold nanowire (AuNW) conductive thin film.[102] Such a film is both transparent and stretchable due to the unique flexible hairy structure of ultrathin AuNWs (2 nm in diameter, aspect ratio >10 000). In addition, the resultant AuNW film could be used as a nanostructured electrode for transparent and stretchable supercapacitors. The entire supercapacitor showed a high transparency of 79% at the wavelength of 550 nm, and could be stretched up to 30% strain without degradation over 80 stretching cycles.

4. Platinum

Due to the unique advantages of Pt including high catalytic ability, chemical stability against oxidation and a high work function of 5.6 eV, it plays an especially important role in microelectronics. The presence of the Pt nanostructures enhances the conductivity of electrons and ions, and consequently gives higher reversible capacitance at high rates. A comparison with previously reported platinum-based materials is given in Table 3.

Zhang *et al.* developed a simple strategy to prepare high-quality platinum nanoparticle (PtNP) decorated graphene for supercapacitors with PtNP uniformly dispersed on the efficiently reduced GO sheets *via* γ-ray irradiation.[103] The PtNP–RGO composites as supercapacitor electrodes displayed a specific capacitance of 154 F g^{-1} at a current density of 0.1 A g^{-1} and the value remained as high as 72.3% at 20 A g^{-1}.

Zhang and co-workers developed a supercapacitor based on graphene/Pt films that showed especially high rate capability (120 F g^{-1} even at 50 A g^{-1}) and cyclability (no attenuation over 10 000 cycles) and peculiar nanosphere morphology after electrochemical cycling.[104] Furthermore, supercapacitors based on the graphene powder with a binder exhibited high specific capacitance (249 F g^{-1} at 0.1 A g^{-1}), long cycle life (no attenuation over 40 000 cycles) and high rate capability (150 F g^{-1} even at 50 A g^{-1}).

Using electrospinning and co-impregnation methods, Lee *et al.* synthesized composite electrodes of MnO_2 and Pt nanophases decorated on the carbon nanofibres (CNFs).[105] Composite MnO_2 and Pt nanophases decorated on the CNFs exhibited superior capacitance (252.3 F g^{-1} at 10 mV s^{-1}), excellent capacitance retention (93.5% after 300 cycles), and high energy densities (13.53–18.06 Wh kg^{-1}). Suryawanshi *et al.* investigated the charge storage capacitive response and field emission behaviour of platinum nanoparticles decorated on carbon nano onions (CNOs), with a specific capacitance of 342.5 F g^{-1} at a scan rate of 100 mV s^{-1}.[106]

Wen *et al.* used a cost-effective atomic layer deposition (ALD) process to prepare core/shell Pt/MnO_2 nanotubes (shown in Fig. 16a).[107] This nanotube-based electrode exhibited high gravimetric and areal specific capacitance (810 F g^{-1} and 75 mF cm^{-2} at a scan rate of 5 mV s^{-1}) as well as an excellent rate capability (68% capacitance retention from 2 to

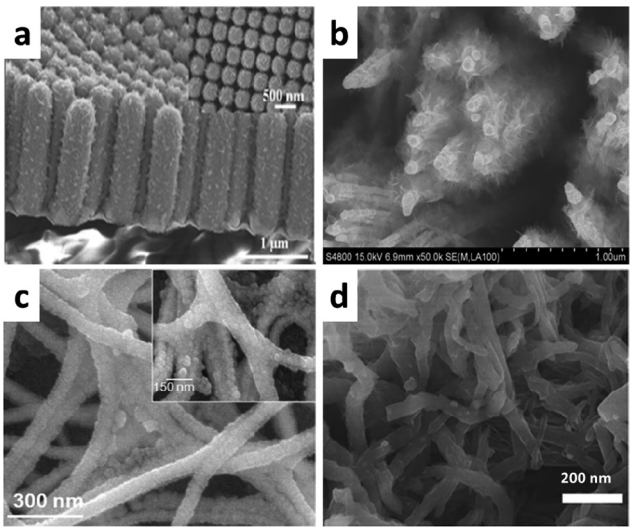

Fig. 16 SEM image of the (a) MnO_2 shell on Pt NTs; (b) Co_3O_4@Pt@MnO_2 NAs; (c) hydrous RuO_2 films coated on Pt nanofiber mats; (d) PANI nanowire network on Pt/CNT yarn. (a) Adapted with permission from ref. 107, © 2014 Wiley; (b) ref. 109, © 2013 Nature; (c) ref. 110, © 2010 The Electrochemical Society; (d) ref. 111, © 2016 The Royal Society of Chemistry.

100 A g^{-1}). Additionally, a negligible capacitance loss was observed after 8000 cycles of random charging–discharging from 2 to 100 A g^{-1}.

Ahn *et al.* investigated the effect of Pt nanostructures on the electrochemical performance of Co_3O_4 electrodes, which were prepared using a co-sputtering system, for micro-electrochemical capacitors.[108] It was shown that the Co_3O_4/Pt nanocomposite electrodes have a capacitance of 391.6 F cm^{-3} at 100 mV s^{-1} along with a superb high-rate performance. Xia *et al.* proposed a novel architectural design of a hierarchical Co_3O_4@Pt@MnO_2 core–shell–shell structure (shown in Fig. 16b) as a high-performance electrode for supercapacitors.[109] The Co_3O_4@Pt@MnO_2 electrode showed several desirable electrochemical features for supercapacitors: a high specific capacitance (497 F g^{-1} by cyclic voltammetry and 539 F g^{-1} by galvanostatic charge–discharge at 1 A g^{-1}), good rate performance (39.6 Wh kg^{-1} at 40 A g^{-1}), and excellent cycling performance (no capacity loss over 5000 cycles).

Choi *et al.* reported the fabrication and characterization of conductive Pt fiber mats as the conducting core of a high rate redox supercapacitor.[110] The Pt fiber mats served as the conducting core for electrochemically deposited hydrous RuO_2 overlayers. The hybrid electrode utilizing hydrous RuO_2-coated Pt fiber mats (shown in Fig. 14c) showed a high specific capacitance of 409.4 F g^{-1} and high rate capability with a capacity loss of only 21.4% from 10 to 1000 mV s^{-1}.

Wang and co-workers successfully designed and fabricated an all-solid-state, highly flexible two-ply yarn supercapacitor based on a Pt/CNT@PANI nanowire nanocomposite material (shown in Fig. 14d).[111] The device demonstrated excellent flexibility and performance, including high capacitance (91.67 mF cm^{-2}), energy density (12.68 μWh cm^{-2}) and excellent cycling stability (80% capacitance retention after 5000 cycles).

Through a simple reflux strategy, Ghouri *et al.* synthesized a crumpled-like TiO_2-Pt/graphene nanocomposite from graphene oxide, $TiCl_3$ and H_2PtCl_6 and employed it as a supercapacitor electrode material.[112] Electrochemical characterization of the introduced nanocomposite indicated that the corresponding specific capacitance was 160 F g^{-1} (at 5 mV s^{-1}) with good stability.

5. Ruthenium

RuO_2 is known as the best electrode material for supercapacitors due to its outstanding specific capacitance and long cycle life. Besides RuO_2, nanocrystalline Ru could also be a promising electrode material for supercapacitors as Juodkazis *et al.* suggested that the theoretical capacitance of Ru is about 3800 F g^{-1} based on the reversible faradaic process as follows:

$$Ru + 3H_2O \leftrightarrow Ru(OH)_3 + 3H^+ + 3e^- \quad (1)$$

Xia *et al.* used nanocrystalline Ru films as electrodes that were deposited on Ni foam by a chemical replacement reaction.[113] The deposited Ru film exhibited a mesoporous structure comprising nanocrystallites and nanopores of 2–3 nm in diameter. A 1.8 V symmetric supercapacitor has been developed by using two Ru thin film electrodes. The Ru//Ru symmetric supercapacitor exhibited a large areal capacitance up to 68 mF cm^{-2} at a current density of 1 mA cm^{-2} and good rate capability. Moreover, no capacitance loss was achieved for the Ru//Ru symmetric supercapacitor after 2000 charge/discharge cycles, indicating excellent cycling performance.

Using $RuCl_3$ and peanut shell-derived MC by a microwave-assisted glycol reduction method, He *et al.* synthesized ruthenium/mesoporous carbon (Ru/MC) composites for supercapacitors.[114] The specific capacitance of the Ru_{20}/MC composites remained 287 F g^{-1} after 1000 cycles. The energy density of the Ru_{20}/MC capacitor only dropped from 10.5 Wh kg^{-1} to 9.8 Wh kg^{-1} with an energy retention of 93.3% after 1000 cycles, showing excellent cycling stability.

By electrospinning and impregnation methods, An *et al.* fabricated nanophase Ru–RuO_2 composites decorated on wrinkled Nb-doped TiO_2 (NTO) nanofibers (NFs).[115] The CV results indicated that the nanophase Ru–RuO_2 composites decorated on the wrinkled NTO NFs possessed a superior capacitance of 496.3 F g^{-1} at 5 mV s^{-1} and good high-rate capacitance.

Lou *et al.* reported the synthesis of stable, highly dispersed ruthenium nanoparticles (RuNPs) on porous activated carbon (PAC) derived from *Moringa Oleifera* fruit shells.[116] The Ru/MOC materials so fabricated exhibited not only superior textural properties but also excellent capacitive properties with extraordinary stability and durability. Upon incorporating RuNPs, the Ru/MOC nanocomposites loaded with a modest amount of metallic Ru (1.0–1.5 wt%) exhibited remarkable

electrochemical and capacitive properties, achieving a maximum capacitance of 291 F g^{-1} at a current density of 1 A g^{-1} in 1.0 M H_2SO_4 electrolyte. The results obtained from a cyclic charge–discharge test showed that the same electrode retained more than 90% of its original capacitance after 2000 consecutive test cycles at 4 A g^{-1}.

6. Palladium

Until now, there is little research on the application of Pd for the supercapacitor, so this may become a hot topic in the future. Palladium decorated C_{60}, MWCNTs, PANI, graphene binary or ternary hybrid materials have been used for supercapacitor applications.[117–120]

Through the electrochemical reduction of solutions containing palladium(II) acetate and C_{60} fullerene, Winkler *et al.* prepared C_{60}/Pd films for supercapacitors, displaying a specific capacitance of 300 F g^{-1}.[117] Giri *et al.* reported a facile method of incorporating palladium nanoparticles into a MWCNT/PANI matrix (shown in Fig. 17a) by *in situ* oxidative polymerization of an aniline monomer.[118] The specific capacitance of the MWCNT/Pd/PANI hybrid was calculated to be 920 F g^{-1} at 2 mV s^{-1} with 87.3% specific capacitance retention over 1000 charge–discharge cycles, indicating excellent cycling stability.

By electrodeposition of polyanilines on palladium nanoparticle loaded TiO_2 nanotubes, Gobal *et al.* prepared PANI/Pd/TiO_2 nanotube (shown in Fig. 17b) electrodes with highly porous structures and good capacitive characteristics.[119] The results illustrated that the specific capacitance of these electrodes was around 1060 F g^{-1} in 1.0 M H_2SO_4 electrolyte as measured at a constant current of 2.0 A g^{-1}. The specific capacitance maintained 94% of the initial value after 10 days of prolonged studies.

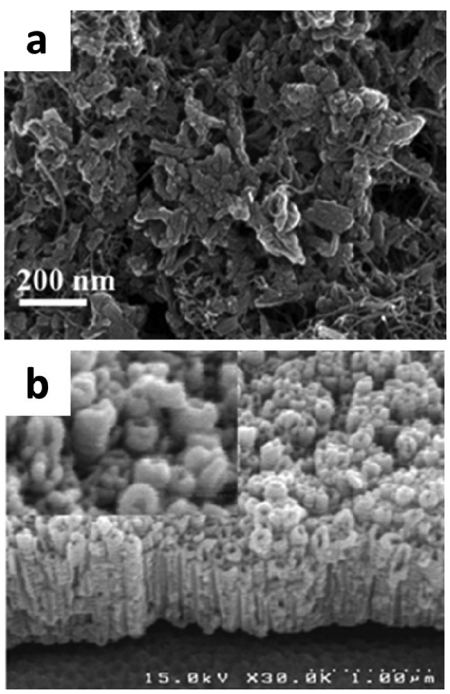

Fig. 17 SEM image of the (a) MWCNT/Pd/PANI hybrid; (b) PANI/Pd/TiO_2 nanotubes. (a) Adapted with permission from ref. 118, © 2013 Springer; (b) ref. 119, © 2013 Elsevier.

Various graphene–Pd composites have been prepared by similar synthetic strategies to those used for the preparation of graphene based Au, Ag and Pt nanostructures. Very recently, Dar *et al.* synthesized a palladium nanoparticle (PdNP) decorated graphene nanosheet (GN) composite *via* a chemical approach in a single step by the simultaneous reduction of graphene oxide and palladium chloride from the aqueous phase using ascorbic acid as a reducing agent.[120] The PdNP-GN composite-based supercapacitor showed remarkable properties with a maximum specific capacitance of 637 F g^{-1}, energy density of 56 Wh kg^{-1} and power density of 1166 W kg^{-1} at a current density of 1.25 A g^{-1}. The fabricated supercapacitor device also exhibits excellent cycle life with 91.4% of the initial specific capacitance retained after 10 000 cycles.

7. Electrode materials containing two kinds of noble metals

The existence of two kinds of noble metals may yield twice the result with half the effort in improving the performance (specific capacitance and cycling stability) of the supercapacitor.

Czerwiński's group used hydrogen electrosorption to fabricate thin electrodeposits of Pd alloys with Pt, Au, and Rh.[121,122] The values of specific capacitance, power density, and energy density were calculated for hydrogen-saturated Pd rich electrodes for temperatures 283–313 K. The best working parameters are exhibited by Pd–Rh alloys with 85–95% Pd, and by Pd–Pt alloys with 90–95% Pd in the bulk. The maximum values of specific capacitance are *ca.* 4500 F g^{-1}, specific energy *ca.* 150 J g^{-1} and specific power up to 750 W g^{-1}.

An *et al.* successfully synthesized CNF composites decorated with Ru–Ag nanophases for use as electrodes in electrochemical capacitors *via* a combination of an electrospinning method and an impregnation method.[123] It gave an excellent capacitance of 350.0 F g^{-1} at 100 mV s^{-1}, superb high-rate performance, and superb capacity retention (98.6%).

By galvanostatic electrodeposition, Zeng and co-workers designed and synthesized a novel three dimensional nanoarchitecture of manganese oxide nanosheets/Pt@nanoporous gold (MnO_x/Pt@NPG) for supercapacitor applications (shown in Fig. 18).[124] Pt nanoparticles which were decorated on NPG not only facilitated the formation of manganese oxide nanosheets, but also improved the conductivity of hybrid electrodes. Besides, the unique nanosheet architecture of MnO_x/Pt@NPG hybrid electrodes allowed high utilization of electrode materials for charge storage with fast ion diffusion between the manganese oxide and the electrolytes and accordingly gave rise to an ultrahigh specific capacitance (775 F g^{-1} at 1 A g^{-1}), low contact resistance and excellent cycling stability.

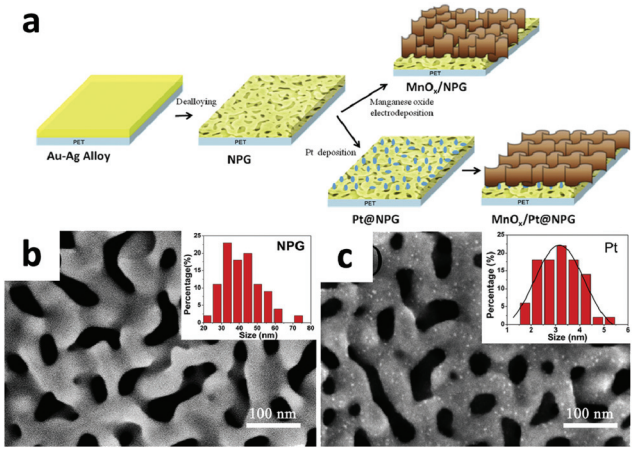

Fig. 18 (a) Schematic illustration of the fabrication process of the MnO_x/NPG and MnO_x/Pt@NPG hybrid electrodes. SEM images of (b) the NPG membrane and (c) the Pt@NPG membrane. The inset of (b) indicates the size distributions of nanoporous channels of the NPG membrane with the mean and standard deviation values of 41 ± 11 nm. The inset of (c) indicates the size distributions of Pt nanoparticles with the mean and standard deviation values of 3 ± 1 nm. Adapted with permission from ref. 123, © 2015 Elsevier.

Very recently, Lee *et al.* introduced a highly stretchable and transparent supercapacitor based on an electrochemically stable Ag–Au core–shell nanowire percolation network electrode.[125] They developed a simple solution process to synthesize the Ag–Au core–shell nanowire with excellent electrical conductivity as well as greatly enhanced chemical and electrochemical stabilities compared to pristine Ag nanowires. The proposed core–shell nanowire-based supercapacitor still possesses fine optical transmittance and outstanding mechanical stability up to 60% strain.

8 Conclusions and outlooks

All in all, supercapacitors have a very broad application prospect.[126–130] Nobel metal-based materials are ideal electrode materials for supercapacitors, because they can improve the specific capacitance and cycling stability of the supercapacitor. Noble metal-doped nanomaterials are expected to improve the conductivity of the electrode material and show a higher specific capacitance by forming electron transfer channels during charge–discharge cycles. Moreover, combining supercapacitor electrode materials such as carbonaceous materials, conductive polymers, and metal oxides with noble metals can significantly improve the electrochemical performance by enhancing their electrical conductivity and charge-storage capability. As noble metals are quite expensive, how to use noble metals to improve the performance of the supercapacitors in a cost-effective way is crucial. In the future, there are some problems to be solved in the application of noble metal-based materials in high-performance supercapacitors. Although enhanced properties have been observed on noble metal-based materials, most of the applications of supercapacitors are limited to the laboratory. Therefore, a lot of work needs to be done, in order to find a general, economical and effective method of fabricating noble metal-based materials for real industrial applications. In order to meet this challenge, the trend of noble metal-based materials in high-performance supercapacitors requires efficient techniques enabling noble metal fabrication in the nano-scale range so as to increase the overall surface-to-volume ratio and hence to reduce the noble metal loading. If we can solve these problems well, the noble metal-based materials will have a very broad application prospect in supercapacitors.

Abbreviation index

AgNP	Silver nanoparticles
NPS	Nanoporous silver
RGO	Reduced graphene oxide
PANI	Polyaniline
PEDOT:PSS	Poly(3,4-ethylenedioxythiophene): poly(styrenesulfonate)
AC	Amorphous carbon
1D	One-dimensional
PVP	Polyvinylpyrrolidone
3D	Three-dimensional
NWs	Nanowires
AAO	Anodic aluminum oxide
CNT	Carbon nanotube
AgNWs	Silver nanowires
MWNTs	Multi-walled nanotubes
SDBS	Dodecylbenzenesulfonate
PPy	Polypyrrole
PAA	Polyacrylic acid
AC	Activated carbon
GNFs	Graphite nanofibers
CFP	Carbon fiber paper
GNS	Graphene nanosheets
pAg	Porous silver
P123	Pluronic P-123
GCE	Glassy carbon electrode
NSP	Nanospikes
MAMNSP	MnO_2/Au/MnO_2 NSP
NMSAS	Nanosized MnO_2 spines on Au stems
NCTs/ANPDM	N-doped carbon-tubes/Au-nanoparticle-doped-MnO_2
SSC	Symmetric supercapacitor
NPAAC	Nanoporous Au/AgO composite
Au-MWCNT	Au-multiwall carbon nanotube
NPG	Nanoporous gold
PMP	Poly(*N*-methyl pyrrole)
PPD	Poly(*p*-phenylenediamine)
GO	Graphene oxide
PtNP	Platinum nanoparticle
CNF	Carbon nanofibres
CNOs	Carbon nano onions

ALD	Atomic layer deposition
MC	Mesoporous carbon
NTO	Nb-doped TiO_2

Acknowledgements

This work is supported by the National Natural Science Foundation of China (Grant 21673203, 21671170), the 333 Project of Jiangsu Province (Grant BRA2011188), the Program for New Century Excellent Talents of the University in China (Grant No. NCET-13-0645), Innovation Scientists and Technicians Troop Construction Projects of Henan Province (164200510018), the program for Innovative Research Team (in Science and Technology) in the University of Henan Province (14IRTSTHN004), the Science & Technology Foundation of Henan Province (122102210253 and 13A150019), sponsored by the Qing Lan Project, Six Talent Plan (2015-XCL-030), Innovation Projects in Jiangsu Province (KYLX16-1385 and SJLX16_0588) and the China Postdoctoral Science Foundation (2012M521115). We also acknowledge the Priority Academic Program Development of Jiangsu Higher Education Institutions and the technical support received at the Testing Center of Yangzhou University.

Notes and references

1 C. Liu, F. Li, L. Ma and H. Cheng, *Adv. Mater.*, 2010, **22**, E28.
2 B.-X. Dong, J. Ge, Y.-L. Teng, J.-J. Gao and L. Song, *J. Mater. Chem. A.*, 2015, **3**, 905.
3 D. Lindley, *Nature*, 2010, **463**, 18.
4 P. Simon and Y. Gogotsi, *Nat. Mater.*, 2008, **7**, 845.
5 M. Chen, W. Li, X. Shen and G. Diao, *ACS Appl. Mater. Interfaces*, 2014, **11**, 4514.
6 M. Wang, J. Han, H. Xiong, R. Guo and Y. Yin, *ACS Appl. Mater. Interfaces*, 2015, **7**, 6909.
7 M. Winter and R. J. Brodd, *Chem. Rev.*, 2004, **104**, 4245.
8 J. Tong, H. Zhang, J. Gu, L. Li, C. Ma, J. Zhao and C. Wang, *J. Mater. Sci.*, 2016, **51**, 1572.
9 D. Larcher and J. M. Tarascon, *Nat. Chem.*, 2015, **7**, 19.
10 H. W. Jang, D. A. Felker, C. W. Bark, Y. Wang, M. K. Niranjan, C. T. Nelson, Y. Zhang, D. Su, C. M. Folkman, S. H. Baek, S. Lee, K. Janicka, Y. Zhu, X. Q. Pan, D. D. Fong, E. Y. Tsymbal, M. S. Rzchowski and C. B. Eom, *Science*, 2011, **331**, 886.
11 X. Dong, Z. Guo, Y. Song, M. Hou, J. Wang, Y. Wang and Y. Xia, *Adv. Funct. Mater.*, 2014, **24**, 3405.
12 S. Biswas and L. T. Drzal, *Chem. Mater.*, 2010, **22**, 5667.
13 B. Dunn, H. Kamath and J. M. Tarascon, *Science*, 2011, **334**, 928.
14 L. Zhang and X. Zhao, *Chem. Soc. Rev.*, 2009, **38**, 2520.
15 G. Wang, L. Zhang and J. Zhang, *Chem. Soc. Rev.*, 2012, **41**, 797.
16 Y. Gogotsi, *Nature*, 2014, **509**, 568.
17 J. Chmiola, G. Yushin, Y. Gogotsi, C. Portet, P. Simon and P. L. Taberna, *Science*, 2006, **313**, 1760.
18 G. L. Soloveichik, *Nature*, 2014, **505**, 163.
19 H. Wang and H. Dai, *Chem. Soc. Rev.*, 2013, **42**, 3088.
20 C. Zhong, Y. Deng, W. Hu, J. Qiao, L. Zhang and J. Zhang, *Chem. Soc. Rev.*, 2015, **44**, 7484.
21 Y. Zhang, Y. Wang, T. Chen, W. Lai, H. Pang and W. Huang, *Chem. Soc. Rev.*, 2015, **44**, 5181.
22 N. S. Malvankar, M. Vargas, K. P. Nevin, A. E. Franks, C. Leang, B. C. Kim, K. Inoue, T. Mester, S. F. Covalla, J. P. Johnson, V. M. Rotello, M. T. Tuominen and D. R. Lovley, *Nat. Nanotechnol.*, 2011, **6**, 573.
23 A. Arico, P. Bruce, B. Scrosati, J. Tarascon and W. Schalkwijk, *Nat. Mater.*, 2005, **4**, 366.
24 L. Yuan, X. Xiao, T. Ding, J. Zhong, X. Zhang, Y. Shen, B. Hu, Y. Huang, J. Zhou and Z. Wang, *Angew. Chem., Int. Ed.*, 2012, **51**, 4934.
25 N. Liu, W. Ma, J. Tao, X. Zhang, J. Su, L. Li, C. Yang, Y. Gao, D. Golberg and Y. Bando, *Adv. Mater.*, 2013, **25**, 4925.
26 Q. Hao, Y. Yu, D. Zhao and C. Xu, *J. Mater. Chem. A*, 2015, **3**, 15944.
27 K. Lee, K. J. Lee, Y. S. Kang, T. J. Shin, Y. Sung and D. Ahn, *Nanoscale*, 2015, **7**, 13860.
28 F. Du, K. Wang, W. Fu, P. Gao, J. Wang, J. Yang and J. Chen, *J. Mater. Chem. A*, 2013, **1**, 13648.
29 S. Li and J. Huang, *J. Mater. Chem. A*, 2015, **3**, 4354.
30 A. F. Holleman and E. Wiberg, *Lehrbuch der Anorganischen Chemie*, Walter de Gruyter, 1985, p. 1486.
31 Y. Wang and I. Zhitomirsky, *Mater. Lett.*, 2011, **65**, 1759.
32 H. Xia, C. Hong, X. Shi, B. Li, G. Yuan, Q. Yao and J. Xie, *J. Mater. Chem. A*, 2015, **3**, 1216.
33 R. Li, X. Liu, H. Wang, Y. Wu and Z. P. Lu, *Electrochim. Acta*, 2015, **182**, 224.
34 Y. Li, H. Fu, Y. Zhang, Z. Wang and X. Li, *J. Phys. Chem. C*, 2014, **118**, 6604.
35 Z. Zeng, P. Sun, J. Zhu and X. Zhu, *RSC Adv.*, 2015, **5**, 17550.
36 J. B. Wu, Z. G. Li and Y. Lin, *Electrochim. Acta*, 2011, **56**, 2116.
37 J. Huang, H. Wu, D. Cao and G. Wang, *Electrochim. Acta*, 2012, **75**, 208.
38 X. Wang, P. Zhang, S. Vongehr, S. Tang, Y. Wang and X. Meng, *RSC Adv.*, 2015, **5**, 45194.
39 Z. Hu, Y. Wang, Y. Xie, Y. Yang, Z. Zhang and H. Wu, *J. Appl. Electrochem.*, 2010, **40**, 341.
40 D. Ghosh, S. Giri, A. Mandal and C. K. Das, *Chem. Phys. Lett.*, 2013, **573**, 41.
41 W. Lan, Y. Sun, Y. Chen, J. Wang, G. Tang, W. Dou, Q. Su and E. Xie, *RSC Adv.*, 2015, **5**, 20878.
42 S. Wang, N. Liu, J. Tao, C. Yang, W. Liu, Y. Shi, Y. Wang, J. Su, L. Lia and Y. Gao, *J. Mater. Chem. A*, 2015, **3**, 2407.
43 Y. Shao, H. Wang, Q. Zhang and Y. Li, *J. Mater. Chem. C*, 2013, **1**, 1245.
44 G. Wee, W. F. Mak, N. Phonthammachai, A. Kiebele, M. V. Reddy, B. V. R. Chowdari, G. Gruner, M. Srinivasan and S. G. Mhaisalkar, *J. Electrochem. Soc.*, 2010, **157**, A179.

45 D. S. Patil, J. S. Shaikh, S. A. Pawar, R. S. Devan, Y. R. Ma, A. V. Moholkar, J. H. Kim, R. S. Kalubarme, C. J. Park and P. S. Patil, *Phys. Chem. Chem. Phys.*, 2012, **14**, 11886.
46 C. A. Amarnath, N. Venkatesan, M. Doble and S. N. Sawant, *J. Mater. Chem. B*, 2014, **2**, 5012.
47 X. Zhang, Z. Lin, B. Chen, W. Zhang, S. Sharma, W. Gu and Y. Deng, *J. Power Sources*, 2014, **246**, 283.
48 A. Singh, Z. Salmi, N. Joshi, P. Jha, P. Decorse, H. Lecoq, S. Lau-Truong, M. Jouini, D. K. Aswal and M. M. Chehimi, *RSC Adv.*, 2013, **3**, 24567.
49 J. Wei, G. Xing, L. Gao, H. Suo, X. He, C. Zhao, S. Lic and S. Xing, *New J. Chem.*, 2013, **37**, 337.
50 J. K. Gan, Y. S. Lim, N. M. Huang and H. N. Lim, *RSC Adv.*, 2015, **5**, 75442.
51 D. S. Patil, S. A. Pawar, R. S. Devan, M. G. Gang, Y. Ma, J. H. Kim and P. S. Patil, *Electrochim. Acta*, 2013, **105**, 569.
52 L. Ma, X. Shen, Z. Ji, G. Zhu and H. Zhou, *Chem. Eng. J.*, 2014, **252**, 95.
53 J. Kim, H. Ju, A. I. Inamdar, Y. Jo, J. Han, H. Kim and H. Im, *Energy*, 2014, **70**, 473.
54 Z. Yu, C. Li, D. Abbitt and J. Thomas, *J. Mater. Chem. A*, 2014, **2**, 10923.
55 S. Nagamuthu, S. Vijayakumar and G. Muralidharan, *Dalton Trans.*, 2014, **43**, 17528.
56 M. Vanitha, K. P. Cao and N. Balasubramanian, *J. Alloys Compd.*, 2015, **644**, 534.
57 J. Zhi, W. Zhao, X. Liu, A. Chen, Z. Liu and F. Huang, *Adv. Funct. Mater.*, 2014, **24**, 2013.
58 C. S. Lee, J. E. Yoo, K. Shin, C. O. Park and J. Bae, *Phys. Status Solidi A*, 2014, **211**, 2890.
59 D. S. Patil, S. A. Pawar, R. S. Devan, S. S. Mali, M. G. Gang, Y. R. Ma, C. K. Hong, J. H. Kim and P. S. Patil, *J. Electroanal. Chem.*, 2014, **724**, 21.
60 S. Dhibar and C. K. Das, *Ind. Eng. Chem. Res.*, 2014, **53**, 3495.
61 K. Kim and S. Park, *Synth. Met.*, 2012, **162**, 2107.
62 M. Sawangphruk, M. Suksomboon, K. Kongsupornsak, J. Khuntilo, P. Srimuk, Y. Sanguansak, P. Klunbud, P. Sukthaa and P. Chiochan, *J. Mater. Chem. A*, 2013, **1**, 9630.
63 P. K. Kalambate, R. A. Dar, S. P. Karna and A. K. Srivastava, *J. Power Sources*, 2015, **276**, 262.
64 H. Adelkhani, K. Didehban and M. Hayasi, *Curr. Appl. Phys.*, 2013, **13**, 522.
65 G. A. Naikoo, R. A. Dar, M. Thomas, M. U. D. Sheikh and F. Khan, *J. Mater. Sci: Mater. Electron.*, 2015, **26**, 2403.
66 J. Kang, A. Hirata, L. Kang, X. Zhang, Y. Hou, L. Chen, C. Li, T. Fujita, K. Akagi and M. Chen, *Angew. Chem., Int. Ed.*, 2013, **52**, 1664.
67 H. Xu, X. Hu, Y. Sun, H. Yang, X. Liu and Y. Huang, *Nano Res.*, 2015, **8**, 1148.
68 W. Si, Ch. Yan, Y. Chen, S. Oswald, L. Han and O. G. Schmidt, *Energy Environ. Sci.*, 2013, **6**, 3218.
69 Y. Gao, H. Jin, Q. Lin, X. Li, M. M. Tavakoli, S. Leung, W. M. Tang, L. Zhou, H. L. W. Chan and Z. Fan, *J. Mater. Chem. A*, 2015, **3**, 10199.
70 Y. Chen, P. Chen, T. Chen, C. Lee and H. Chiu, *J. Mater. Chem. A*, 2013, **1**, 13301.
71 Y. Dai, S. Tang, X. Wang, X. Huang, C. Zhu, Z. Hang and X. Meng, *Chem. Lett.*, 2014, **43**, 122.
72 Z. Zeng, X. Long, H. Zhou, E. Guo, X. Wang and Z. Hu, *Electrochim. Acta*, 2015, **163**, 107.
73 J.-S. Liu and Y. Hu, *Int. J. Electrochem. Sci.*, 2013, **8**, 9231.
74 T. Qiu, B. Luo, M. Giersig, E. M. Akinoglu, L. Hao, X. Wang, L. Shi, M. Jin and L. Zhi, *Small*, 2014, **10**, 4136.
75 B. Qu, L. Hu, Y. Chen, C. Li, Q. Li, Y. Wang, W. Wei, L. Chen and T. Wang, *J. Mater. Chem. A*, 2013, **1**, 7023.
76 S. Liu, S. Guo, S. Sun and X. You, *Nanoscale*, 2015, **7**, 4890.
77 J. Xu, C. Wang, Ji. Liu, S. Xu, W. Zhang and Y. Lu, *RSC Adv.*, 2015, **5**, 38995.
78 J. Zhu, Z. Xun and B. Lu, *Nano Energy*, 2014, **7**, 114.
79 S. Kim, P. Thiyagarajan and J. Jang, *Nanoscale*, 2014, **6**, 11646.
80 S.-I. Kim, S.-W. Kim, K. Jung, J.-B. Kim and J.-H. Jang, *Nano Energy*, 2016, **24**, 17.
81 K. N. Chaudhari, S. Chaudhari and J. Yu, *J. Electroanal. Chem.*, 2016, **761**, 98.
82 B. Ankamwar, P. Das and U. K. Sur, *Indian J. Phys.*, 2016, **4**, 391.
83 Z. Yu, S. Sun and M. Huang, *Int. J. Electrochem. Sci.*, 2016, **11**, 3643.
84 S. Mandal, A. Pal, R. K. Arun and N. Chanda, *J. Electroanal. Chem.*, 2015, **755**, 22.
85 X. Lang, L. Zhang, T. Fujita, Y. Ding and M. Chen, *J. Power Sources*, 2012, **197**, 325.
86 H. Hu, K. Zhang, S. Li, S. Jia and C. Ye, *J. Mater. Chem. A*, 2014, **2**, 20916.
87 K. Zhang, H. Hu, W. Yao and C. Ye, *J. Mater. Chem. A*, 2015, **3**, 617.
88 B. N. Reddy, N. Billa and M. Deepa, *ChemPlusChem*, 2012, **77**, 789.
89 Q. Lv, S. Wang, H. Sun, J. Luo, J. Xiao, J. Xiao, F. Xiao and S. Wang, *Nano Lett.*, 2016, **16**, 40.
90 L. Wang, T. Wu, S. Du, M. Pei, W. Guo and S. Wei, *RSC Adv.*, 2016, **6**, 1004.
91 V. Veeramani, B. Dinesh, S. Chen and R. Saraswathi, *J. Mater. Chem. A*, 2016, **4**, 3304.
92 A. L. M. Reddy, M. M. Shaijumon, S. R. Gowda and P. M. Ajayan, *J. Phys. Chem. C*, 2010, **114**, 658.
93 X. Han, S. Liu, Y. Yuan, Y. Wang and L. Hu, *J. Alloys Compd.*, 2012, **543**, 200.
94 J. S. Shayeh, A. Ehsani, M. R. Ganjali, P. Norouzi and B. Jaleh, *Appl. Surf. Sci.*, 2015, **353**, 594.
95 X. Zhang, Y. Xu, Y. Ma, M. Yang and Y. Qi, *Eur. J. Inorg. Chem.*, 2015, **22**, 3764.
96 X. Zheng, X. Yan, Y. Sun, Z. Bai, G. Zhang, Y. Shen, Q. Liang and Y. Zhang, *ACS Appl. Mater. Interfaces*, 2015, **7**, 2480.
97 X. Lu, T. Zhai, X. Zhang, Y. Shen, L. Yuan, B. Hu, L. Gong, J. Chen, Y. Gao, J. Zhou, Y. Tong and Z. L. Wang, *Adv. Mater.*, 2012, **24**, 938.
98 P. Wang, H. Liu, Q. Tan and J. Yang, *RSC Adv.*, 2014, **4**, 42839.

99 Q. Lv, H. Sun, X. Li, J. Xiao, F. Xiao, L. Liu, J. Luo and S. Wang, *Nano Energy*, 2016, **21**, 39.
100 S. Duan and R. Wang, *NPG Asia Mater.*, 2014, **6**, e122.
101 X. Y. Lang, H. T. Yuan, Y. Iwasa and M. W. Chen, *Scr. Mater.*, 2011, **64**, 923.
102 S. Gong, Y. Zhao, Q. Shi, Y. Wang, L. W. Yap and W. Cheng, *Electroanalysis*, 2016, **28**, 1298.
103 Q. Zhang, Y. Zhang, Z. Gao, H. Ma, S. Wang, J. Peng, J. Lia and M. Zhai, *J. Mater. Chem. C*, 2013, **1**, 321.
104 D. Zhang, X. Zhang, Y. Chen, C. Wang, Y. Ma, H. Dong, L. Jiang, Q. Meng and W. Hu, *Phys. Chem. Chem. Phys.*, 2012, **14**, 10899.
105 Y. Lee, G. An and H. Ahn, *J. Nanosci. Nanotechnol.*, 2015, **15**, 8931.
106 S. R. Suryawanshi, V. Kaware, D. Chakravarty, P. S. Walke, M. A. More, K. Joshi, C. S. Rout and D. J. Late, *RSC Adv.*, 2015, **5**, 80990.
107 L. Wen, Y. Mi, C. Wang, Y. Fang, F. Grote, H. Zhao, M. Zhou and Y. Lei, *Small*, 2014, **10**, 3162.
108 H. Ahn and T. Seong, *J. Alloys Compd.*, 2009, **478**, L8.
109 H. Xia, D. Zhu, Z. Luo, Y. Yu, X. Shi, G. Yuan and J. Xie, *Sci. Rep.*, 2013, **3**, 2978.
110 S. Choi, T. Hyun, H. Lee, S. Jang, S. Oh and I. Kim, *Electrochem. Solid-State Lett.*, 2010, **13**, A65.
111 Q. Wang, Y. Wu, T. Li, D. Zhang, M. Miao and A. Zhang, *J. Mater. Chem. A*, 2016, **4**, 3828.
112 Z. K. Ghouri, N. A. M. Barakat, P. S. Saud, M. Park, B.-S. Kim and H. Y. Kim, *J. Mater. Sci: Mater. Electron.*, 2016, **27**, 3894.
113 H. Xia, B. Li and L. Lu, *RSC Adv.*, 2014, **4**, 11111.
114 X. He, K. Xie, R. Li and M. Wu, *Mater. Lett.*, 2014, **115**, 96.
115 H. L. An, Y. Lee and H. Ahn, *Res. Chem. Intermed.*, 2015, **41**, 4785.
116 B.-S. Lou, P. Veerakumar, S.-M. Chen, V. Veeramani, R. Madhu and S.-B. Liu, *Sci. Rep.*, 2016, **6**, 19949.
117 K. Winkler, E. Grodzka, F. D'Souza and A. L. Balch, *J. Electrochem. Soc.*, 2007, **154**, K1.
118 S. Giri, D. Ghosh, A. Malas and C. K. Das, *J. Electron. Mater.*, 2013, **8**, 2595.
119 F. Gobal and M. Faraji, *J. Electroanal. Chem.*, 2013, **691**, 51.
120 R. A. Dar, L. Giri, S. P. Karna and A. K. Srivastava, *Electrochim. Acta*, 2016, **196**, 547.
121 M. Łukaszewski, A. Zurowski and A. Czerwiński, *J. Power Sources*, 2008, **185**, 1598.
122 M. Łukaszewski, K. Hubkowska, U. Koss and A. Czerwiński, *J. Solid State Electrochem.*, 2012, **16**, 2533.
123 G. An and H. Ahn, *ECS Solid State Lett.*, 2013, **2**, M33.
124 Z. Zeng, H. Zhou, X. Long, E. Guo and X. Wang, *J. Alloys Compd.*, 2015, **632**, 376.
125 H. Lee, S. Hong, J. Lee, Y. D. Suh, J. Kwon, H. Moon, H. Kim, J. Yeo and S. H. Ko, *ACS Appl. Mater. Interfaces*, 2016, **8**, 15449.
126 L. Mi, Y. Gao, S. Cui, H. Hou and W. Chen, *Inorg. Chem. Front.*, 2014, **1**, 745.
127 J. Zhao, J. He, M. Sun, M. Qu and H. Pang, *Inorg. Chem. Front.*, 2015, **2**, 129.
128 S. Chen, M. Xue, Y. Li, Y. Pan, L. Zhu, D. Zhang, Q. Fang and S. Qiu, *Inorg. Chem. Front.*, 2015, **2**, 177.
129 B. Li, M. Zheng, H. Xue and H. Pang, *Inorg. Chem. Front.*, 2016, **3**, 175.
130 Y. Yan, H. Xu, W. Guo, Q. Huang, M. Zheng, H. Pang and H. Xue, *Inorg. Chem. Front.*, 2016, **3**, 791.